Québécoisation Method for the Pricing of Parisian Options with Jump Risk*

Marc Chesney† Nikola Vasiljević‡

December 15, 2015

Abstract

In this paper, a new technique for pricing of European and American Parisian options, that we call the québécoisation method, is developed. We study the pricing of Parisian options in a hyper-exponential jump-diffusion model using the double Laplace-Carson transform with respect to the time to maturity and the residual Parisian time (time to expiration of the Parisian window) of the system of two partial integro-differential equations describing the option price dynamics. The transformed, i.e., québécoised, option price and hedging parameters delta and gamma are computed in a closed form, and the final results are obtained via the two-dimensional Gaver-Stehfest inversion algorithm. Our pricing method is analytically tractable, and it provides important economic insights for pricing and hedging of European and American Parisian options in the presence of jumps.

Keywords: Parisian options, Québécoisation method, Gaver-Stehfest inversion algorithm, Hyper-exponential jump-diffusion model.

Mathematics Subject Classification (2010): 60G51, 35E15, 60G40, 62L15.

JEL classification: G13, C02, C65.

*We would like to thank Jérôme Detemple, João Pedro Vidal Nunes, Paola Pederzoli, and Felix Stang for their valuable comments. We are also thankful to the participants at Gerzensee Research Days 2014, and at Bachelier Finance Conference 2014 in Brussels, Belgium. We gratefully acknowledge financial support from the Swiss Finance Institute (SFI) and the Department for Banking and Finance (DBF) at the University of Zurich (UZH). The previous version of this paper was entitled "European and American Parisian options in a jump-diffusion model".

†University of Zurich and Swiss Finance Institute, Plattenstrasse 32, 8032 Zurich, Switzerland; e-mail: marc.chesney@bf.uzh.ch.

‡Corresponding author. University of Zurich and Swiss Finance Institute, Plattenstrasse 14, 8032 Zurich, Switzerland; e-mail: nikola.vasiljevic@bf.uzh.ch.

1 Introduction

In the last couple of decades, proliferate research in quantitative finance provided the necessary mathematical tools for pricing and hedging of a wide range of financial products. In addition to vanilla European and American options, many different types of exotic options are presently traded at organized exchanges and over-the-counter (OTC). Indeed, it is widely recognized that standard put and call options do not perfectly match all risk profiles, hence they do not provide universally suitable means of hedging.

Standard (one-touch) barrier options are among the most popular exotic derivative contracts. These options have identical features to those of its vanilla counterparts except that they additionally depend on whether or not the underlying asset process reaches a certain predefined region during the life of the option. An option that is cancelled (activated) when the barrier is breached for the first time is referred to it as a knock-out (knock-in) option. By construction, barrier options are particularly suitable for investors who have a directional view on the market. They provide the same upside potential as the corresponding vanilla option, but they are less expensive due to knock-out (knock-in) feature. Moreover, barrier options might be attractive to those market participants who are seeking for a protection against possible adverse market moves above or below certain threshold level. However, since knock-out (knock-in) events are triggered as soon as the underlying asset price reaches the barrier, they also create incentives for manipulation of the underlying asset price. Influential market participants might be able to move the price of the underlying asset close to the barrier, and therefore to trigger the cancellation (activation) of certain knock-out (knock-in) option contracts. Clearly, the issues associated with the enforced triggering of standard barrier option provisions and clauses are particularly pronounced in illiquid markets.

To mitigate this problem, Chesney, Jeanblanc and Yor (1997) introduced a class of occupation-time derivatives called Parisian (barrier) options. Compared to standard (one-touch) barrier options, Parisian-style derivatives introduce the notion of the occupation time, i.e., the time that the underlying asset price spends with or without interruption in a certain region (e.g., below or above a threshold level). Therefore, Parisian options are *not* knocked-out (knocked-in) immediately as the cancellation (activation) region is reached. Instead, the underlying asset price has to spend a certain amount of time, called Parisian window, in the excursion region. Market participants who could possibly benefit from a directional move towards or away from the barrier would have to be able to deliberately keep the price above or below the barrier for the pre-specified amount of time, i.e., the Parisian window. Since it is more difficult to sustain control over the underlying price process for an extended period of time, holders of Parisian options are better protected from potential adverse actions of option writers, and vice versa. Therefore, the

introduction of Parisian provisions provides a remedy for a potential price manipulation. Moreover, it mitigates the problem of discontinuous standard barrier option's Greeks near the threshold level, which is important for the risk management of derivative instruments.

Continuous monitoring of the underlying asset price process naturally introduces the notion of a "clock" or a "stopwatch" that is triggered or stopped depending on the barrier event(s) and measures the time spent in the excursion region. More specifically, one can distinguish between two different types of Parisian-style options. A standard Parisian option, or simply a Parisian option, is characterized by a clock which records the duration of uninterrupted excursions. The Parisian clock is activated (reset to zero) each time the underlying process crosses the barrier and enters (exits) the excursion region. On the other hand, a cumulative Parisian option, which is also known as a Par*asian* option, is characterized by a clock that is never reset to zero. Therefore, the Par*asian* clock measures the total time that the underlying process spends in the excursion region.

The main goal of this paper is to study the pricing of European and American (standard) Parisian options in a jump-diffusion model. Sudden market moves during the the recent financial and economic turmoil and the Financial crisis of 2007–08 have reiterated the importance of jump risk for modelling of asset returns. Therefore, in times of increased uncertainty, mathematical models of financial markets have to account for a possibility of large adverse moves in asset returns. Lévy models, which are able of capturing such dynamics, represent an attractive framework for financial applications. We consider a class of Lévy models called hyper-exponential jump-diffusion models (HEM), which are introduced in Lipton (2002). Any Lévy process with completely monotone Lévy density can be approximated by a HEM model (e.g., see Crosby, Le Saux and Mijatović (2010) and Jeannin and Pistorius (2010)). In particular, our modelling framework encompasses a broad range of popular Lévy processes, e.g., VG, NIG, Generalized Hyperbolic, and CGMY. Additionally, the double-exponential model (DEM) of Kou (2002) belongs to the hyper-exponential class as well. Last but not least, option pricing in a HEM setting is analytically tractable, which makes these models particularly interesting for financial engineering applications.

A substantial progress has already been made in the pricing of standard and cumulative Parisian options.[1] Nevertheless, it is the European-style Parisian payoff structure that attracted the most attention. With the notable exception of Haber, Schönbucher and Wilmott (1999), American Parisian options have been considered only in Chesney and Gauthier (2006) who studied the valuation problem using the decomposition technique

[1] E.g., see Chesney et al. (1997), Zhu and Stokes (1998),Avellaneda and Wu (1999), Haber, Schönbucher and Wilmott (1999), Hugonnier (1999), Vetzal and Forsyth (1999), Costabile (2002), Fujita and Miura (2002),Schröder (2003), Bernard, Le Courtois and Quitard-Pinon (2005), Chesney and Gauthier (2006), Anderluh and van der Weide (2009), Labart and Lelong (2009), Albrecher, Kortschak and Zhou (2012), and Zhu and Chen (2013).

similar to that of Kim (1990), Jacka (1991), and Carr, Jarrow and Myneni (1992)(for vanilla American options), and Gao, Huang and Subrahmanyam (2000) (for American one-touch barrier options). However, no closed-form solution is provided in the case of finite-maturity American Parisian options. Furthermore, the vast majority of literature on the pricing and the hedging of Parisian options assumes a Black-Scholes setting. To the best of our knowledge, the only paper which studies Parisian options in a jump-diffusion framework is Albrecher, Kortschak and Zhou (2012). Some other types of occupation-time derivatives in the presence of jump risk are analyzed in Cai, Chen and Wan (2010). Nevertheless, both papers consider only a double-exponential jump-diffusion model.

Our contribution to the literature on the pricing of Parisian options is twofold. First, we consider the most general modelling framework in the context of Parisian option pricing, both European and American-style. Second, this paper pioneers the research on pricing of American Parisian options in a jump-diffusion setting. Our approach is based on the double Laplace-Carson transform of the system of partial integro-differential equations (PIDEs) with respect to the time to maturity and the residual Parisian time, which leads to a system of ordinary integro-differential equations (OIDEs) that can be solved in a closed form. Parisian option price and Greek letters delta and gamma are then computed using a two-dimensional Gaver-Stehfest inversion algorithm. Therefore, by construction, our solution procedure represents an extension of the (single-maturity) randomization method, i.e., canadization, introduced in finance by Carr (1998). Since our "double canadization" approach is motivated by the Parisian option pricing problem, we intermingle the two geographic terms and christen our method *québécoisation*, deriving its name from the term *Québécois* that refers to a French-speaking person of the Canadian province of Québéc.

The rest of the paper is organized as follows. An overview of the HEM model and the symmetry relations for Parisian options is presented in Section 2. The PIDE systems for European and American Parisian up-and-out put options are analyzed in Section 3. We introduce the québécoisation method and derive analytical results for québécoised European and American Parisian up-and-out put options in Section 4, and we show some numerical examples of Parisian option prices and the Greeks. In Section 6 we study the effects of jumps on Parisian options. Finally, Section 7 concludes, and the proofs are given in the Appendix.

2 Preliminaries

2.1 Hyper-exponential jump-diffusion model

We introduce a filtered probability space $(\Omega, \mathcal{F}, \mathbb{F} = \{\mathcal{F}_t, t \geq 0\}, \mathbb{Q})$ which satisfies the usual assumptions. Since we are interested in option pricing, our starting point is the risk-neutral dynamics of the underlying asset which is given by a hyper-exponential jump-diffusion process

$$\frac{dS_t}{S_{t^-}} = (r - \delta - \lambda\zeta)dt + \sigma dW_t + d\left(\sum_{i=1}^{N_t}(V_i - 1)\right). \tag{1}$$

Therefore, the filtration is defined as $\mathcal{F}_t = \sigma(W_s, N_s; s \leq t, \{V_j\})$. The process $\{W_t, t \geq 0\}$ represents a standard Brownian motion under the risk-neutral measure $\mathbb{Q}$. The (domestic) risk-free interest rate is denoted by $r \in \mathbb{R}^+$, the dividend yield (or the foreign risk-free interest rate in the case of foreign exchange options) is $\delta \in \mathbb{R}_0^+$, and the volatility parameter is $\sigma \in \mathbb{R}^+$. Jumps are modelled by a Poisson process $\{N_t, t \geq 0\}$ with jump intensity parameter $\lambda \in \mathbb{R}_0^+$. The probability density function (p.d.f.) characterizing the sequence of independent and identically distributed (i.i.d.) hyper-exponential random variables $\{Y_i := \log(V_i) : i = 1, 2, ...\}$ is given by

$$\varphi_Y(y) = \sum_{i=1}^{m} p_i \eta_i e^{-\eta_i y} \mathbb{1}_{\{y \geq 0\}} + \sum_{j=1}^{n} q_j \theta_j e^{\theta_j y} \mathbb{1}_{\{y < 0\}}, \tag{2}$$

where probabilities of different kinds of positive and negative jumps (conditional on jump occurrence) are given by $p_i > 0$ for $i = 1, ..., m$ and $q_j > 0$ for $j = 1, ..., n$, respectively. The conditional probabilities sum up to unity, i.e., $\sum_{i=1}^{m} p_i + \sum_{j=1}^{n} q_j = 1$. Jump size parameters $\eta_i > 1$ for $i = 1, ..., m$ and $\theta_j > 0$ for $j = 1, ..., n$ correspond to different kinds of discontinuous upward and downward movements, respectively. The symbol $\mathbb{1}_{\{\cdot\}}$ denotes an indicator function.

Applying the Itô lemma one can obtain the dynamics of the log-price $X_t := \log S_t$ in the form

$$X_t := X_0 + \mu t + \sigma W_t + \sum_{i=1}^{N_t} Y_i, \quad X_0 := \log S_0. \tag{3}$$

The drift of the log-price process is defined as

$$\mu := r - \delta - \lambda\zeta - \frac{\sigma^2}{2}, \tag{4}$$

and the average size of a return jump is given by

$$\zeta := \mathbb{E}\left[e^{Y_1} - 1\right] = \sum_{i=1}^{m} \frac{p_i \eta_i}{\eta_i - 1} + \sum_{j=1}^{n} \frac{q_j \theta_j}{\theta_j + 1} - 1. \tag{5}$$

A very important mathematical object for our analysis is the cumulant generating function (c.g.f.). In the case of an HEM process, the c.g.f. is given by

$$\begin{aligned} \Psi(a) :&= \frac{1}{t} \log \mathbb{E}\left[e^{aX_t} | X_0 = 0\right] \\ &= \frac{\sigma^2 a^2}{2} + \mu a + \lambda \left(\sum_{i=1}^{m} \frac{p_i \eta_i}{\eta_i - a} + \sum_{j=1}^{n} \frac{q_j \theta_j}{\theta_j + a} - 1 \right), \end{aligned} \tag{6}$$

for any $a \in (-\theta_1, \eta_1)$. Without loss of generality we assume that $\eta_1 < \eta_2 < \cdots < \eta_m$ and $\theta_1 < \theta_2 < \cdots < \theta_n$. The characteristic equation, which is defined as

$$\Psi(x) = \alpha, \quad \text{for } \alpha > 0, \tag{7}$$

has exactly $(m+1)$ positive real roots $\{\beta_{i,\alpha}\}_{i=1,\ldots,m+1}$ and $(n+1)$ negative real roots $\{\gamma_{j,\alpha}\}_{j=1,\ldots,n+1}$ such that $-\infty < \gamma_{n+1,\alpha} < -\theta_n < \gamma_{n,\alpha} < -\theta_{n-1} < \cdots < \gamma_{2,n} < -\theta_1 < \gamma_{1,\alpha} < 0 < \beta_{1,\alpha} < \eta_1 < \beta_{2,\alpha} < \cdots < \eta_{m-1} < \beta_{m,\alpha} < \eta_m < \beta_{m+1,\alpha} < +\infty$ (e.g., see Lemma 2.1 in Cai (2009), pp. 128–129). The special cases of geometric Brownian motion of Black and Scholes (1973), spectrally one-sided Lévy models considered in Avram, Chan and Usabel (2002), or double-exponential jump-diffusion model of Kou (2002), allow for computation of the respective characteristic roots in a closed-form. More involved HEM models, i.e., jump-diffusion specifications beyond DEM model, require solving higher order polynomial equations, which can be attained only numerically.

Last but not least, the infinitesimal generator of the Markovian process X_t introduced in equation (3) is defined as

$$\begin{aligned} (\mathcal{L}v)(x) :&= \lim_{t \downarrow 0} \frac{\mathbb{E}[v(X_t) | X_0 = x] - v(x)}{t} \\ &= \frac{\sigma^2}{2} \frac{\partial^2 v}{\partial x^2}(x) + \mu \frac{\partial v}{\partial x}(x) + \lambda \int_{-\infty}^{+\infty} [v(x+y) - v(x)] \varphi_Y(y) dy, \end{aligned} \tag{8}$$

where $v(\cdot)$ is any twice continuously differentiable function.

2.2 Symmetry and parity relations in the presence of jumps

Parisian options come in many different flavors. Depending on the exercise style, we can distinguish between European and American Parisian call and put options. Furthermore,

there exist "knock-in" and "knock-out" options, as well as "up" and "down" features. Therefore, it is possible to construct 32 different combinations in total. Clearly, our goal is not to present results for all existing types of Parisian options. In fact, Chesney, Jeanblanc and Yor (1997), Section 6 and Section 7, pp. 176–179, and Chesney and Gauthier (2006), Section 2.1, p. 478, show that there exist symmetry and parity relations between different option types, hence it is enough to consider only several cases to span the entire list of Parisian option contracts. However, their results hold only in the Black-Scholes setting. We generalize these findings and provide the symmetry and parity relations for Parisian options in a hyper-exponential jump-diffusion model.

We start our analysis with an example of symmetry relations for USD/EUR foreign exchange European and American Parisian options. The risk-neutral dynamics of the spot exchange rate S_t is assumed to take the form (1). The strike price is K, the barrier level is H, the option contract matures at time T, and the Parisian window is denoted by D. The crucial observation is that holding a USD/EUR put option is equivalent to a long position in an appropriately chosen number of EUR/USD calls. This symmetry applies to vanilla European and American options, as well as to European and American standard barrier and Parisian options (e.g., see Chesney, Jeanblanc and Yor (1997) and Chesney and Gauthier (2006)). Therefore, if we denote a European (American) call and put by c and p (C and P), respectively, we obtain the following symmetry relations

$$\begin{aligned} p(S_t, K, r, \delta, T; \sigma, \nu) &= S_t K \cdot c(1/S_t, 1/K, \delta, r, T; \sigma, \tilde{\nu}), \\ P(S_t, K, r, \delta, T; \sigma, \nu) &= S_t K \cdot C(1/S_t, 1/K, \delta, r, T; \sigma, \tilde{\nu}). \end{aligned} \tag{9}$$

The set of parameters $\nu := \{\lambda, \{p_i, \eta_i\}_{i=1,\ldots,m}, \{q_j, \theta_j\}_{j=1,\ldots,n}\}$ describes a compensated compound Poisson process with hyper-exponential jumps under the risk-neutral measure $\mathbb{Q}$. On the other hand, the set of jump parameters $\tilde{\nu} := \{\tilde{\lambda}, \{\tilde{p}_i, \tilde{\eta}_i\}_{i=1,\ldots,m}, \{\tilde{q}_j, \tilde{\theta}_j\}_{j=1,\ldots,n}\}$ is computed under the equivalent martingale measure $\tilde{\mathbb{Q}}$ which ensures that the discounted and reinvested price process $\{e^{-(r-\delta)t} S_t, t \geq 0\}$ is a martingale. The change of measure for a hyper-exponential jump-diffusion model is based on the Esscher transform. The explicit expressions for HEM parameters under the equivalent martingale measure $\tilde{\mathbb{Q}}$ are provided in **?**, Appendix B, pp. 652–653.

The put-call symmetry relations for European and American Parisian options in the HEM model are therefore obtained by putting together the symmetry results for Parisian

options in the Black-Scholes setting and the equation (9):

$$\begin{aligned}
\mathcal{O}^p_{do}(S_t, K, H, r, \delta, T, D; \sigma, \nu) &= S_t K \cdot \mathcal{O}^c_{uo}(1/S_t, 1/K, 1/H, \delta, r, T, D; \sigma, \tilde{\nu}),\\
\mathcal{O}^p_{di}(S_t, K, H, r, \delta, T, D; \sigma, \nu) &= S_t K \cdot \mathcal{O}^c_{ui}(1/S_t, 1/K, 1/H, \delta, r, T, D; \sigma, \tilde{\nu}),\\
\mathcal{O}^p_{uo}(S_t, K, H, r, \delta, T, D; \sigma, \nu) &= S_t K \cdot \mathcal{O}^c_{do}(1/S_t, 1/K, 1/H, \delta, r, T, D; \sigma, \tilde{\nu}),\\
\mathcal{O}^p_{ui}(S_t, K, H, r, \delta, T, D; \sigma, \nu) &= S_t K \cdot \mathcal{O}^c_{di}(1/S_t, 1/K, 1/H, \delta, r, T, D; \sigma, \tilde{\nu}).
\end{aligned} \tag{10}$$

The introduced notation has the following meaning. The option type is denoted by $\mathcal{O} \in \{\pi, \Pi\}$. The letter π designates a European Parisian option contract, and the letter Π stands for an American Parisian option. The first letter in the subscript is either d or u, and it corresponds to down or up barrier feature, respectively. The second letter in the subscript can be either i (knock-in option) or o (knock-out option). Finally, the superscript provides the information about the exercise style of the option, and we use the letter c for calls and the letter p for puts. For example, π^p_{do} stands for a European Parisian down-and-out put option.

Last but not least, European-style Parisian options satisfy in-out parity relations. The sum of a knock-in and knock-out European Parisian options (with otherwise identical contractual specifications) is equal to their vanilla European counterpart. Therefore, for European Parisian put options it holds that

$$\begin{aligned}
\pi^p_{do}(S_t, K, H, r, \delta, T, D; \sigma, \nu) + \pi^p_{di}(S_t, K, H, r, \delta, T, D; \sigma, \nu) &= p(S_t, K, r, \delta, T; \sigma, \nu),\\
\pi^p_{uo}(S_t, K, H, r, \delta, T, D; \sigma, \nu) + \pi^p_{ui}(S_t, K, H, r, \delta, T, D; \sigma, \nu) &= p(S_t, K, r, \delta, T; \sigma, \nu).
\end{aligned} \tag{11}$$

Similar in-out parity relations hold also for European Parisian call options.

3 PIDE systems for Parisian put options

In this section, we introduce the systems of partial integro-differential equations describing the evolution of European and American Parisian put options. Our approach to the construction of PIDE systems for Parisian options hinges on the work of Haber, Schönbucher and Wilmott (1999) and Zhu and Chen (2013). We contribute by generalizing their results to a (finite-activity) jump-diffusion setting. In particular, we study Parisian up-and-out put options. Results for up-and-in put options can be derived analogously, and the prices of certain Parisian call options can be obtained with the help of symmetry and parity relations introduced in Section 2.2. We focus on one type of Parisian options to keep our analysis relatively simple and tractable.

The following notation is used in the rest of the paper. The option contract expires at time T, and the Parisian window is given by D. The strike price is given by K, and the

barrier level is H $(K < H)$. At any point it time $t(0 \leq t \leq T)$ the price of the underlying asset is given by S_t, and the early exercise price (for American Parisian option) is denoted by B_t. The log-price, the log-strike, the log-barrier, and the log-early exercise price are defined as $x := \log S_t$, $\kappa := \log K$, $h := \log H$, and $b := \log B_t$, respectively. Without loss of generality, our analysis assumes that the rebate is equal to zero.

3.1 European Parisian put options

European Parisian up-and-out put option price is a function of the log-price x, the calendar time t, and the Parisian time t_p. The state variable t_p measures uninterrupted time that the underlying process spends above the boundary, i.e., the duration of the underlying process's uninterrupted excursion above the barrier H. The Parisian time is therefore characterized by

$$\begin{cases} t_p = 0, \quad dt_p = 0, & \text{for} \quad x < h, \\ dt_p = dt, & \text{for} \quad x \geq h. \end{cases} \tag{12}$$

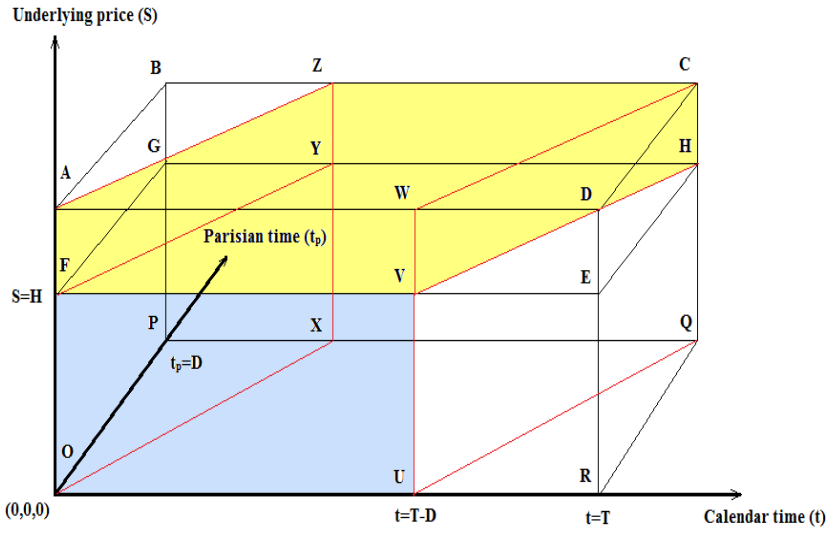

Figure 1: Pricing domains of European Parisian up-and-out put option.

Following Haber, Schönbucher and Wilmott (1999), we first define the pricing domain as the parallelepiped ADCBPORQ in Figure 1. By definition, the occupation time t_p is always less or equal than the calendar time t, hence we exclude the prism ABZXOP from the pricing domain. Furthermore, the Parisian provision matters as long as the remaining time to maturity is greater than the residual Parisian time. When $T - t \leq D - t_p$ the

occupation time condition becomes void and the price of a Parisian up-and-out put option becomes equal to the price of its vanilla counterpart. Therefore, the prism CDWUQR should also be excluded. Both modifications of the original pricing domain are thoroughly discussed in Zhu and Chen (2013), Section 2, pp. 876–880.

The *excursion region*, i.e., the region in which the Parisian clock is activated, is defined as

$$\mathscr{E} := \big\{h \leq x < \infty, \quad t_p \leq t \leq t_p + T - D, \quad 0 \leq t_p \leq D\big\}, \tag{13}$$

and it is represented by the parallelepiped AZCWVFYH in Figure 1. On the other hand, in the *standard region* the Parisian clock is inactive, and the option price depends only on the calendar time. Thus, the standard region is given by

$$\mathscr{S} := \big\{-\infty < x < h, \quad 0 \leq t \leq T - D, \quad t_p = 0\big\}, \tag{14}$$

and it is represented by the rectangle OFVU. Moreover, the region $\mathscr{S}$ can be decomposed into two subregions. The *payoff region* is the subspace of the standard region in which the option is in-the-money, i.e.,

$$\mathscr{S}_p := \big\{-\infty < x < \kappa, \quad 0 \leq t \leq T - D, \quad t_p = 0\big\}. \tag{15}$$

On the other hand, the *corridor region* represents the subspace of the standard region in which the option is out-the-money

$$\mathscr{S}_c := \big\{\kappa \leq x < h, \quad 0 \leq t \leq T - D, \quad t_p = 0\big\}. \tag{16}$$

European Parisian up-and-out put price is then decomposed as

$$\pi_{uo}(x,t,t_p) = \begin{cases} \pi^e_{uo}(x,t,t_p), & \text{if } \ (x,t,t_p) \in \mathscr{E}, \\ \pi^s_{uo}(x,t), & \text{if } \ (x,t,t_p) \in \mathscr{S}. \end{cases} \tag{17}$$

In the standard region $\mathscr{S}$, the option price satisfies the PIDE

$$\frac{\partial \pi_{uo}}{\partial t}(x,t,t_p) + \mathcal{L}\pi_{uo}(x,t,t_p) = r\pi_{uo}(x,t,t_p). \tag{18}$$

The operator $\mathcal{L}$ is defined in (8). The terminal and the boundary condition in the standard region are, respectively,

$$\begin{aligned} &\lim_{t \uparrow T-D} \pi^s_{uo}(x,t) = p(x,D), \\ &\lim_{x \downarrow -\infty} \pi^s_{uo}(x,t) = e^{-r(T-D-t)} \lim_{x \downarrow -\infty} p(x,D) = Ke^{-r(T-D-t)}. \end{aligned} \tag{19}$$

The function $p(x,D) := p(x,D;\kappa)$ represents the price of a vanilla European put option

with log-strike κ and maturity D. In addition, a value matching and a smooth pasting condition, respectively, are imposed at the boundary between payoff region $\mathscr{S}_p$ and the corridor region $\mathscr{S}_c$, i.e., for $x = \kappa$,

$$\begin{aligned} \lim_{x\uparrow\kappa} \pi^s_{uo}(x,t) &= \lim_{x\downarrow\kappa} \pi^s_{uo}(x,t), \\ \lim_{x\uparrow\kappa} \frac{\partial \pi^s_{uo}}{\partial x}(x,t) &= \lim_{x\downarrow\kappa} \frac{\partial \pi^s_{uo}}{\partial x}(x,t). \end{aligned} \tag{20}$$

In the excursion region, the option price satisfies the PIDE

$$\frac{\partial \pi_{uo}}{\partial t}(x,t,t_p) + \frac{\partial \pi_{uo}}{\partial t_p}(x,t,t_p) + \mathcal{L}\pi_{uo}(x,t,t_p) = r\pi_{uo}(x,t,t_p). \tag{21}$$

The terminal and the boundary condition in the excursion region are, respectively,

$$\begin{aligned} \lim_{t_p\uparrow D} \pi^e_{uo}(x,t,t_p) &= 0, \\ \lim_{x\uparrow+\infty} \pi^e_{uo}(x,t,t_p) &= 0. \end{aligned} \tag{22}$$

Finally, to close the system of PIDEs we impose a value matching and a smooth pasting condition at the boundary between the standard and the excursion region (for $x = h$):

$$\begin{aligned} \lim_{x\uparrow h} \pi^s_{uo}(x,t) &= \lim_{x\downarrow h} \pi^e_{uo}(x,t,t_p), \\ \lim_{x\uparrow h} \frac{\partial \pi^s_{uo}}{\partial x}(x,t) &= \lim_{x\downarrow h} \frac{\partial \pi^e_{uo}}{\partial x}(x,t,t_p). \end{aligned} \tag{23}$$

The PIDE system for European Parisian up-and-out put option is difficult to solve analytically. However, we proceed along the lines of Zhu and Chen (2013), Section 3.1, pp. 881–882, and simplify our problem and transform the three-dimensional into a two-dimensional PIDE in the excursion region by rotating the time-coordinate system. Since the calendar and the Parisian clock in the excursion region are ticking at the same rate, the partial derivatives of the option price with respect to the calendar time t and Parisian time t_p in (21) can be replaced by a directional derivative with respect to a new time variable t_h. In other words, we introduce the transformation

$$\mathcal{R}_e : \quad \frac{\partial}{\partial t} + \frac{\partial}{\partial t_p} \quad \longrightarrow \quad \sqrt{2}\, \frac{\partial}{\partial t_h}. \tag{24}$$

The new clock measures time t_h, and it is ticking at the rate which is $\sqrt{2}$ times higher than the one associated with the calendar clock t and the Parisian clock t_p. We normalize the ticking rate in the excursion region by rescaling the new clock. This is achieved by substituting t_h with $t'_h := t_h/\sqrt{2}$. The time dependence in the excursion region is now

fully captured by a new time variable, i.e., the hybrid excursion time t_e, which is given by

$$t_e := t'_h \mathbb{1}_{\{X_t \geq h\}}. \tag{25}$$

Furthermore, the transformation $\mathcal{R}_e$ introduces a new time variable in the standard region, i.e., the standard time t_s, which is defined as

$$t_s := t\mathbb{1}_{\{X_t < h\}} + t_l \mathbb{1}_{\{X_t \geq h\}}, \tag{26}$$

where t_l represents the last exit time from the standard region

$$t_l := \begin{cases} 0, & \text{if } \big\{0 \leq u \leq t \big| X_u < h\big\} = \emptyset, \\ \sup\limits_{0 \leq u \leq t} \big\{u \big| X_u < h\big\}, & \text{otherwise.} \end{cases} \tag{27}$$

The variable t_s runs as the normal calendar time t in the standard region. On the other hand, it is merely a parameter in the excursion region. The standard clock is stopped (but not reset) as soon as the underlying process enters the excursion region, and it is equal to the last exit time t_l (before the calendar time t) from the standard region. If the process reverts to the region $\mathscr{S}$, the clock t_s immediately jumps to the calendar time and starts ticking again. On the other hand, the hybrid excursion clock is reset to zero whenever the underlying process leaves the region $\mathscr{E}$.

We adjust the notation due to the time transformation $\mathcal{R}_e$ and the resulting separation of time variables arising from the symmetrical treatment of the calendar and the Parisian clock. The excursion region and the two standard subregions, respectively, are now defined as

$$\begin{cases} \tilde{\mathscr{E}} & := \big\{h \leq x < \infty, \;\; t_s = t_l, \;\; 0 \leq t_e \leq D\big\}, \\ \tilde{\mathscr{S}_c} & := \big\{\kappa \leq x < h, \;\; 0 \leq t_s \leq T - D, \;\; t_e = 0\big\}, \\ \tilde{\mathscr{S}_p} & := \big\{-\infty < x < \kappa, \;\; 0 \leq t_s \leq T - D, \;\; t_e = 0\big\}. \end{cases} \tag{28}$$

The price of a European Parisian up-and-out put option is then given by

$$\tilde{\pi}_{uo}(x, t_s, t_e) = \begin{cases} \tilde{\pi}^e_{uo}(x, t_e), & \text{if } \; (x, t_s, t_e) \in \tilde{\mathscr{E}}, \\ \tilde{\pi}^s_{uo}(x, t_s), & \text{if } \; (x, t_s, t_e) \in \tilde{\mathscr{S}}. \end{cases} \tag{29}$$

Consequently, the option price dynamics in the standard and the excursion region is described by a two-dimensional PIDE system

$$\begin{cases} \dfrac{\partial \tilde{\pi}_{uo}}{\partial t_e}(x, t_s, t_e) + \mathcal{L}\tilde{\pi}_{uo}(x, t_s, t_e) = r\tilde{\pi}_{uo}(x, t_s, t_e), & \text{if } \; (x, t_s, t_e) \in \tilde{\mathscr{E}}, \\ \dfrac{\partial \tilde{\pi}_{uo}}{\partial t_s}(x, t_s, t_e) + \mathcal{L}\tilde{\pi}_{uo}(x, t_s, t_e) = r\tilde{\pi}_{uo}(x, t_s, t_e), & \text{if } \; (x, t_s, t_e) \in \tilde{\mathscr{S}}. \end{cases} \tag{30}$$

The corresponding terminal and boundary conditions in the standard region $\tilde{\mathscr{S}}$ become

$$\begin{aligned}
\lim_{t_s \uparrow T-D} \tilde{\pi}^s_{uo}(x, t_s) &= p(x, 0; \kappa, D), \\
\lim_{x \downarrow -\infty} \tilde{\pi}^s_{uo}(x, t_s) &= K e^{-r(T-D-t_s)}, \\
\lim_{x \uparrow \kappa} \tilde{\pi}^s_{uo}(x, t_s) &= \lim_{x \downarrow \kappa} \tilde{\pi}^s_{uo}(x, t_s), \\
\lim_{x \uparrow \kappa} \frac{\partial \tilde{\pi}^s_{uo}}{\partial x}(x, t_s) &= \lim_{x \downarrow \kappa} \frac{\partial \tilde{\pi}^s_{uo}}{\partial x}(x, t_s).
\end{aligned} \tag{31}$$

The terminal and the boundary conditions in the excursion region $\tilde{\mathscr{E}}$ are now given by

$$\begin{aligned}
\lim_{t_e \uparrow D} \tilde{\pi}^e_{uo}(x, t_e) &= 0, \\
\lim_{x \uparrow +\infty} \tilde{\pi}^e_{uo}(x, t_e) &= 0.
\end{aligned} \tag{32}$$

Finally, the value matching and the smooth pasting conditions at the boundary between the standard and the excursion region are

$$\begin{aligned}
\lim_{x \uparrow h} \tilde{\pi}^s_{uo}(x, t_s) &= \lim_{x \downarrow h} \tilde{\pi}^e_{uo}(x, t_e = 0), \\
\lim_{x \uparrow h} \frac{\partial \tilde{\pi}^s_{uo}}{\partial x}(x, t_s) &= \lim_{x \downarrow h} \frac{\partial \tilde{\pi}^e_{uo}}{\partial x}(x, t_e = 0).
\end{aligned} \tag{33}$$

3.2 American Parisian put options

The early exercise feature of American-style options, which is also known in the literature as the free boundary problem, brings in an additional layer of complexity; e.g., see Detemple (2005) and Jeanblanc, Yor and Chesney (2009). More specifically, one distinguishes between a continuation region where the early exercise is suboptimal and the option holder prefers to keep the contract, and an (early) exercise region in which the option holder prefers to immediately exercise the contract and collect the proceeds thereupon. The two regions are separated by a (non-linear) early exercise boundary which is not known in advance and has to be determined as part of the solution.

The time transformation discussed in the previous section applies also to American Parisian up-and-out put options because, other things being equal, the boundary between the standard and the excursion region is not affected by the early exercise feature. In other words, the excursion and the corridor region defined in (13) and (16) remain the same. Therefore, the transformation (24) holds also for American Parisian options, and we can directly consider the simplified PIDE system.

First, the early exercise feature changes the structure of the standard region. More specifically, the payoff region (15) splits into two subspaces. The *payoff continuation*

region is defined as

$$\tilde{\mathscr{S}}_{pc} := \big\{ b(t_s) < x < \kappa, \quad 0 \le t_s \le T - D, \quad t_e = 0 \big\}, \tag{34}$$

and the *payoff exercise region* is given by

$$\tilde{\mathscr{S}}_{pe} := \big\{ -\infty < x \le b(t_s), \quad 0 \le t_s \le T - D, \quad t_e = 0 \big\}. \tag{35}$$

Furthermore, we denote the standard continuation region (which includes the corridor and the payoff continuation subregions) by $\tilde{\mathscr{S}}^* := \tilde{\mathscr{S}}_c \cup \tilde{\mathscr{S}}_{pc} = \tilde{\mathscr{S}} \setminus \tilde{\mathscr{S}}_{pe}$. Then, the price of an American Parisian up-and-out put option is decomposed as

$$\tilde{\Pi}_{uo}(x, t_s, t_e) = \begin{cases} \tilde{\Pi}^e_{uo}(x, t_e), & \text{if } \ (x, t_s, t_e) \in \tilde{\mathscr{E}}, \\ \tilde{\Pi}^s_{uo}(x, t_s), & \text{if } \ (x, t_s, t_e) \in \tilde{\mathscr{S}}^*, \\ e^{\kappa} - e^{x}, & \text{if } \ (x, t_s, t_e) \in \tilde{\mathscr{S}}_{pe}. \end{cases} \tag{36}$$

The early exercise boundary divides the payoff region into subregions (34) and (35), i.e.,

$$b(t_s) := \sup \big\{ x \mid \tilde{\Pi}^s_{uo}(x, t_s) = e^{\kappa} - e^{x} \big\}. \tag{37}$$

The dynamics of an American Parisian up-and-out put option is therefore described by the following PIDEs in the standard continuation region $\tilde{\mathscr{S}}^*$ and in the excursion region $\tilde{\mathscr{E}}$, respectively:

$$\begin{cases} \dfrac{\partial \tilde{\Pi}_{uo}}{\partial t_e}(x, t_s, t_e) + \mathcal{L}\tilde{\Pi}_{uo}(x, t_s, t_e) = r\tilde{\Pi}_{uo}(x, t_s, t_e), & \text{if } \ (x, t_s, t_e) \in \tilde{\mathscr{E}}, \\ \dfrac{\partial \tilde{\Pi}_{uo}}{\partial t_s}(x, t_s, t_e) + \mathcal{L}\tilde{\Pi}_{uo}(x, t_s, t_e) = r\tilde{\Pi}_{uo}(x, t_s, t_e), & \text{if } \ (x, t_s, t_e) \in \tilde{\mathscr{S}}^*. \end{cases} \tag{38}$$

The value matching and the smooth pasting conditions at the boundary between the standard continuation and the standard payoff region are given by

$$\begin{aligned} \lim_{x \downarrow b(t_s)} \tilde{\Pi}^s(x, t_s) &= e^{\kappa} - e^{b(t_s)}, \\ \lim_{x \downarrow b(t_s)} \frac{\partial \tilde{\Pi}^s}{\partial x}(x, t_s) &= -e^{b(t_s)}. \end{aligned} \tag{39}$$

The terminal condition in the standard continuation region $\tilde{\mathscr{S}}^*$ is

$$\lim_{t_s \uparrow T - D} \tilde{\Pi}^s_{uo}(x, t_s) = P(x, D), \tag{40}$$

where $P(x, D) := P(x, D; \kappa)$ represents the price of a vanilla American put option with

the log-strike κ and the maturity D. The boundary conditions in this region are

$$\begin{aligned} \lim_{t_e \uparrow D} \tilde{\Pi}^e_{uo}(x, t_e) &= 0, \\ \lim_{x \uparrow +\infty} \tilde{\Pi}^e_{uo}(x, t_e) &= 0. \end{aligned} \tag{41}$$

Finally, the value matching and the smooth pasting conditions at the boundary between the standard continuation and the excursion region are

$$\begin{aligned} \lim_{x \uparrow h} \tilde{\Pi}^s(x, t_s) &= \lim_{x \downarrow h} \tilde{\Pi}^e(x, t_e = 0) \\ \lim_{x \uparrow h} \frac{\partial \tilde{\Pi}^s}{\partial x}(x, t_s) &= \lim_{x \downarrow h} \frac{\partial \tilde{\Pi}^e}{\partial x}(x, t_e = 0). \end{aligned} \tag{42}$$

4 Pricing Parisian put options

In this section, we first recall the definition of (single) Laplace-Carson transform (LCT) and briefly explain the idea behind the canadization method for the pricing of vanilla and standard barrier options. Subsequently, we introduce the double Laplace-Carson transform (DLCT) and the québécoisation method for the pricing of Parisian options. Finally, we derive the main theoretical result of our paper, i.e., the closed-form solutions for québécoised European and American Parisian up-and-out put options.

4.1 From Canadization to Québécoisation method

For any locally integrable function $f : \mathbb{R}^+ \to \mathbb{R}$ and for all $\alpha \in \mathbb{R}^+$ the Laplace-Carson transform is defined as

$$\left(\mathscr{LC}\right)_z [f(z)](\alpha) := \check{f}(\alpha) := \alpha \int_0^{+\infty} e^{-\alpha z} f(z) dz. \tag{43}$$

Once the transform is computed (either numerically or analytically), the original function can be evaluated using the Gaver-Stehfest inversion algorithm (GS) given by

$$f_M(z) = \sum_{k=1}^{2M} \varsigma_{k,M} \check{f}\left(\frac{k \log(2)}{z}\right), \quad M \in \mathbb{N}, \tag{44}$$

where $\lfloor a \rfloor$ is defined as the greatest number $a' \in \mathbb{N}$ such that $a' \leq a$. This formula already includes the linear Salzer convergence acceleration scheme. The summation coefficients

are given by

$$\varsigma_{k,M} := \frac{(-1)^{M+k}}{k} \sum_{j=\lfloor (k+1)/2 \rfloor}^{\min\{k,M\}} \frac{j^{M+1}}{M!} \binom{M}{j} \binom{2j}{j} \binom{j}{k-j}. \tag{45}$$

In the limit $M \to \infty$, the approximation $f_M(z)$ converges to the true value of the original function, i.e.,

$$\lim_{M \to \infty} f_M(z) = f(z). \tag{46}$$

The proof of the convergence of the Gaver-Stehfest algorithm is provided in **?**.

Canadized options are defined as options whose time to maturity is an exponentially distributed random variable. Therefore, it follows from equation (43) that the price of a canadized option is an LCT of the original option price w.r.t. the time to maturity. Due to the memoryless property of the exponential class of distributions, an LCT of a PIDE describing the option price dynamics eliminates the time dependence. This implies that the original pricing problem reduces to the one of solving an OIDE, which is analytically tractable.

Generalization of equation (43) to the case of double, i.e., two-dimensional, Laplace-Carson transform is straightforward. For $\alpha_1, \alpha_2 \in \mathbb{R}^+$ and a locally integrable function $g : \mathbb{R}^+ \times \mathbb{R}^+ \to \mathbb{R}$, the double Laplace-Carson transform is defined as

$$\begin{aligned} \left(\mathscr{DLC}\right)_{z_1,z_2} [g(z_1,z_2)](\alpha_1,\alpha_2) &:= \hat{g}(\alpha_1,\alpha_2) \\ &:= \alpha_1\alpha_2 \int_0^{+\infty} e^{-\alpha_2 z_2} \int_0^{+\infty} e^{-\alpha_1 z_1} g(z_1,z_2) dz_1 dz_2. \end{aligned} \tag{47}$$

Following Abate and Whitt (2006), Section 3 and Section 4, pp. 413–414, a DLCT can be computed by successively applying two one-dimensional LCTs:

$$\begin{aligned} \check{g}(\alpha_1, z_2) &:= \alpha_1 \int_0^{+\infty} e^{-\alpha_1 z_1} g(z_1,z_2) dz_1, \\ \hat{g}(\alpha_1,\alpha_2) &:= \alpha_2 \int_0^{+\infty} e^{-\alpha_2 z_2} \check{g}(\alpha_1,z_2) dz_2. \end{aligned} \tag{48}$$

Similarly, the inversion is carried through a two-step procedure. For given values of z_1 and z_2, we first invert the function $\hat{g}(\alpha_1,\alpha_2)$ w.r.t. the second argument, while we keep the first argument constant. Thus, we obtain the function $\check{g}(\alpha_1, z_2)$. Subsequently, we conduct the inversion w.r.t. the first argument of the function $\check{g}(\alpha_1, z_2)$. The procedure

can be summarized as follows:

$$\begin{aligned} \check{g}_N(\alpha_{1,m}, z_2) &:= \sum_{n=1}^{2N} \varsigma_{n,N} \hat{g}(\alpha_{1,m}, \alpha_{2,n}), \\ g_{M,N}(z_1, z_2) &:= \sum_{m=1}^{2M} \varsigma_{m,M} \check{g}_N(\alpha_{1,m}, z_2), \end{aligned} \tag{49}$$

where $\alpha_{1,m} := m\log(2)/z_1$ $(m = 1, 2, ..., 2M,\ M \in \mathbb{N})$ and $\alpha_{2,n} := n\log(2)/z_2$ $(n = 1, 2, ..., 2N,\ N \in \mathbb{N})$. The coefficients $\varsigma_{m,M}$ and $\varsigma_{n,N}$ are defined in equation (45). The two-dimensional Gaver-Stehfest inversion algorithm yields an approximation $g_{M,N}(z_1, z_2)$ of the original function's true value $g(z_1, z_2)$. In the limit, when M and N become very large, the following convergence result holds

$$\lim_{M,N\to\infty} g_{M,N}(z_1, z_2) = g(z_1, z_2). \tag{50}$$

This result is a direct consequence of (46). It is important to stress out that the inner loop is crucial for the overall accuracy of the method, i.e., the intermediary function $\check{g}_N(\alpha_{1,m}, z_2)$ has to be computed with sufficient accuracy in order to obtain satisfactory results in the outer loop. Therefore, a general recommendation is to impose the condition $M < N$; e.g., see Choudhury, Lucantoni and Whitt (1997). Section 8, pp. 461–462. However, Abate and Whitt (2006), Section 8, pp. 418–419, show that the case $M = N$ is good enough for many applications, and we follow their recommendation in our implementations.

Definition 1.
A québécoised option is a Parisian-style option whose time to maturity and residual Parisian time are exponentially distributed.

It follows from the equations (47)–(48) and the definition above that the price of a québécoised option can be computed as a DLCT of the price of a Parisian option w.r.t. the two time variables. The québécoisation approach simplifies the pricing problem for Parisian option by transforming the PIDE system into an OIDE system, which can be solved in a closed form. The original price is then obtained via the two-dimensional Gaver-Stehfest algorithm described in equation (49). In the case of American Parisian options, we emphasize that the québécoised early exercise boundary is flat because the transformed option price is a time-independent function. This is another consequence of the memorylessness of exponential distributions. Finally, the results of Kimura (2010), Corollary 3.1, p. 177, for the Greeks of canadized vanilla European and American options can be easily generalized to the case of québécoised European and American Parisian Greeks. More specifically, québécoised delta and gamma can be computed as the first and the second-order derivatives of the québécoised option prices w.r.t. the underlying asset price.

Other types of single and double Laplace transform, e.g., Euler and Talbot algorithm, are discussed in Abate and Whitt (2006).

4.2 Québécoised European and American Parisian up-and-out put option

Theorem 1 (**Pricing of Québécoised European Parisian up-and-out put options**).
Assume that the asset price process $\{S_u, t \leq u \leq T\}$ *is described by the hyper-exponential model* (1)–(2). *Consider a European Parisian up-and-out put option introduced in Section 3.1.*

(a) In the excursion region, the québécoised option price is given by

$$\hat{\hat{\pi}}^e_{uo}(x, \alpha^e_{k_e}) = \sum_{j=1}^{n+1} A^-_j e^{\gamma_{j,r+\alpha^e_{k_e}}(x-h)}. \tag{51}$$

(b) In the corridor region, the québécoised option price is given by

$$\begin{aligned}\hat{\hat{\pi}}^s_{uo}(x, \alpha^s_{k_s}) = &\sum_{i=1}^{m+1} B^+_i e^{\beta_{i,r+\alpha^s_{k_s}}(x-h)} + \sum_{j=1}^{n+1} B^-_j e^{\gamma_{j,r+\alpha^s_{k_s}}(x-h)} \\ &+ \sum_{k_v=1}^{2N} \varsigma_{k_v,N} \sum_{j=1}^{n+1} \overline{\omega}'_{j,k_v} e^{\gamma_{j,r+\alpha^v_{k_v}}(x-\kappa)}.\end{aligned} \tag{52}$$

(c) In the payoff region, the québécoised option price is given by

$$\begin{aligned}\hat{\hat{\pi}}^s_{uo}(x, \alpha^s_{k_s}) = &\sum_{i=1}^{m+1} C^+_i e^{\beta_{i,r+\alpha^s_{k_s}}(x-\kappa)} + \sum_{k_v=1}^{2N} \varsigma_{k_v,N} \sum_{i=1}^{m+1} \underline{\omega}'_{i,k_v} e^{\beta_{i,r+\alpha^v_{k_v}}(x-\kappa)} \\ &+ \sum_{k_v=1}^{2N} \varsigma_{k_v,N} \left(\frac{\alpha^s_{k_s}}{\alpha^s_{k_s}+r} \frac{\alpha^v_{k_v}}{\alpha^v_{k_v}+r} e^{\kappa} - \frac{\alpha^s_{k_s}}{\alpha^s_{k_s}+\delta} \frac{\alpha^v_{k_v}}{\alpha^v_{k_v}+\delta} e^{x} \right).\end{aligned} \tag{53}$$

The parameters $\{\alpha^v_{k_v}\}_{k_v=1,2,\ldots,2N}$ *are defined as* $\alpha^v_{k_v} := k_v \log(2)/D$. *The parameters* $\{\alpha^s_{k_s}\}_{k_s=1,2,\ldots,2M_s}$ *and* $\{\alpha^e_{k_e}\}_{k_e=1,2,\ldots,2M_e}$ *are* $\alpha^s_{k_s} := k_s \log(2)/(T-D-t_s)$ *and* $\alpha^s_{k_e} := k_e \log(2)/(D-t_e)$, *respectively. Positive and negative roots of the characteristic equation* $\Psi(u) = r + \alpha^\rho_{k_\rho}$, *where* $\rho \in \{v, e, s\}$, *are denoted by* $\{\beta_{i,r+\alpha^\rho_{k_\rho}}\}_{i=1,2,\ldots,m+1}$ *and* $\{\gamma_{j,r+\alpha^\rho_{k_\rho}}\}_{j=1,2,\ldots,n+1}$, *respectively. The Lévy exponent* $\Psi(\cdot)$ *is defined in* (6), *and the Gaver-Stehfest coefficients are defined in equation* (45). *The coefficients* $\{A^-_j\}_{j=1,\ldots,n+1}$,

$\{B_i^+\}_{i=1,...,m+1}$, $\{B_j^-\}_{j=1,...,n+1}$, *and* $\{C_i^+\}_{i=1,...,m+1}$ *solve the system of linear equations*

$$\mathbf{P}\mathbf{u}_e = \mathbf{p}_e, \tag{54}$$

where $\mathbf{u}_e := (A_1^-, ..., A_{n+1}^-, B_1^+, ..., B_{m+1}^+, B_1^-, ..., B_{n+1}^-, C_1^+, ..., C_{m+1}^+)'$, $\mathbf{p}_e$ *is a (2m+2n+4)-dimensional column vector, and* $\mathbf{P}$ *is a (2m+2n+4)-dimensional square matrix. The elements of the vector* $\mathbf{p}_e$ *and the matrix* $\mathbf{P}$ *are given in the appendix.*

The price of an American-style option can be written as a sum of the corresponding European-style option and the early exercise premium; e.g., see Kim (1990), Jacka (1991), and Carr, Jarrow and Myneni (1992). In particular, American Parisian up-and-out put option value can be decomposed in the form

$$\tilde{\Pi}_{uo}(x, t_s, t_e) = \tilde{\pi}_{uo}(x, t_s, t_e) + \tilde{\epsilon}_{uo}(x, t_s, t_e). \tag{55}$$

From expressions (29), (36) and (55) it follows that the early exercise premium of an American Parisian up-and-out put option is given by

$$\tilde{\epsilon}_{uo}(x, t_s, t_e) = \begin{cases} \tilde{\epsilon}^e_{uo}(x, t_e), & \text{if } (x, t_s, t_e) \in \tilde{\mathscr{E}}, \\ \tilde{\epsilon}^s_{uo}(x, t_s), & \text{if } (x, t_s, t_e) \in \tilde{\mathscr{S}}^*, \\ e^\kappa - e^x - \tilde{\pi}^s_{uo}(x, t_s), & \text{if } (x, t_s, t_e) \in \tilde{\mathscr{S}}_{pe}. \end{cases} \tag{56}$$

Therefore, from the PIDE systems for European and American Parisian up-and-out put options, we deduce the dynamics of the corresponding Parisian early exercise premium in the form

$$\begin{cases} \dfrac{\partial \tilde{\epsilon}_{uo}}{\partial t_e}(x, t_s, t_e) + \mathcal{L}\tilde{\epsilon}_{uo}(x, t_s, t_e) = r\tilde{\epsilon}_{uo}(x, t_s, t_e), & \text{if } (x, t_s, t_e) \in \tilde{\mathscr{E}}, \\ \dfrac{\partial \tilde{\epsilon}_{uo}}{\partial t_s}(x, t_s, t_e) + \mathcal{L}\tilde{\epsilon}_{uo}(x, t_s, t_e) = r\tilde{\epsilon}_{uo}(x, t_s, t_e), & \text{if } (x, t_s, t_e) \in \tilde{\mathscr{S}}^*. \end{cases} \tag{57}$$

The value matching and the smooth pasting conditions at the boundary between the standard continuation and the standard payoff region are, respectively,

$$\begin{aligned} \lim_{x \downarrow b(t_s)} \tilde{\epsilon}^s_{uo}(x, t_s) &= e^\kappa - e^{b(t_s)} - \tilde{\pi}^s_{uo}(x, t_s)\big|_{x=b(t_s)}, \\ \lim_{x \downarrow b(t_s)} \frac{\partial \tilde{\epsilon}^s_{uo}}{\partial x}(x, t_s) &= -e^{b(t_s)} - \frac{\partial \tilde{\pi}^s_{uo}}{\partial x}(x, t_s)\Big|_{x=b(t_s)}. \end{aligned} \tag{58}$$

The terminal conditions for the early exercise premium in the regions $\tilde{\mathscr{E}}$ and $\tilde{\mathscr{S}}^*$ are, respectively,

$$\begin{aligned} \lim_{t_e \uparrow D} \tilde{\epsilon}^e_{uo}(x, t_e) &= 0, \\ \lim_{t_s \uparrow T-D} \tilde{\epsilon}^s_{uo}(x, t_s) &= \epsilon_p(x, D), \end{aligned} \tag{59}$$

where $\epsilon_p(x,D) := P(x,D) - p(x,D)$ is the vanilla early exercise premium. The boundary condition in the excursion region is

$$\lim_{x\uparrow+\infty} \tilde{\epsilon}^e_{uo}(x,t_e) = 0. \tag{60}$$

Finally, the value matching and the smooth pasting condition at boundary between the standard continuation and the excursion region are respectively given by

$$\begin{aligned} \lim_{x\uparrow h} \tilde{\epsilon}^s_{uo}(x,t_s) &= \lim_{x\downarrow h} \tilde{\epsilon}^e_{uo}(x,t_e=0), \\ \lim_{x\uparrow h} \frac{\partial \tilde{\epsilon}^s_{uo}}{\partial x}(x,t_s) &= \lim_{x\downarrow h} \frac{\partial \tilde{\epsilon}^e_{uo}}{\partial x}(x,t_e=0). \end{aligned} \tag{61}$$

Theorem 2 (**Pricing of Québécoised American Parisian up-and-out put options**).
Assume that the asset price process $\{S_u, t \le u \le T\}$ *is described by the hyper-exponential model* (1)–(2). *Consider an American Parisian up-and-out put option introduced in Section 3.2.*

(a) In the excursion region, the québécoised early exercise premium is given by

$$\hat{\tilde{\epsilon}}^e_{uo}(x,\alpha^e_{k_e}) = \sum_{j=1}^{n+1} D_j^- e^{\gamma_{j,r+\alpha^e_{k_e}}(x-h)}. \tag{62}$$

(b) In the standard continuation region, the québécoised early exercise premium is given by

$$\begin{aligned} \hat{\tilde{\epsilon}}^s_{uo}(x,\alpha^s_{k_s}) = &\sum_{i=1}^{m+1} F_i^+ e^{\beta_{i,r+\alpha^s_{k_s}}(x-h)} + \sum_{j=1}^{n+1} F_j^- e^{\gamma_{j,r+\alpha^s_{k_s}}(x-h)} \\ &+ \sum_{k_v=1}^{2N} \varsigma_{k_v,N} \sum_{j=1}^{n+1} \phi'_{j,k_v} e^{\gamma_{j,r+\alpha^v_{k_v}}(x-\hat{b})}. \end{aligned} \tag{63}$$

(c) In the payoff exercise region, the québécoised early exercise premium is given by

$$\hat{\tilde{\epsilon}}^s_{uo}(x,\alpha^s_{k_s}) = e^{\kappa} - e^x - \hat{\tilde{\pi}}^s_{uo}(x,\alpha^s_{k_s}). \tag{64}$$

The parameters $\{\alpha^v_{k_v}\}_{k_v=1,2,\ldots,2N}$, $\{\alpha^s_{k_s}\}_{k_s=1,2,\ldots,2M_s}$, *and* $\{\alpha^e_{k_e}\}_{k_e=1,2,\ldots,2M_e}$, *the coefficients* $\{\beta_{i,r+\alpha^\rho_{k_\rho}}\}_{i=1,2,\ldots,m+1}$ *and* $\{\gamma_{j,r+\alpha^\rho_{k_\rho}}\}_{j=1,2,\ldots,n+1}$ *for* $\rho \in \{v,e,s\}$, *the Lévy exponent. and the Gaver-Stehfest coefficients are defined in Theorem 1. The coefficients*

$\{D_j^-\}_{j=1,...,n+1}$, $\{F_i^+\}_{i=1,...,m+1}$, *and* $\{F_j^-\}_{j=1,...,n+1}$ *solve the system of linear equations*

$$\mathbf{Q}\mathbf{u}_a = \mathbf{p}_a, \tag{65}$$

where $\mathbf{u}_a := (D_1^-, ..., D_{n+1}^-, F_1^+, ..., F_{m+1}^+, F_1^-, ..., F_{n+1}^-)'$, $\mathbf{p}_a$ *is a (m+2n+3)-dimensional column vector, and* $\mathbf{Q}$ *is a (m+2n+3)-dimensional square matrix. The elements of the vector* $\mathbf{p}_a$ *and the matrix* $\mathbf{Q}$*, as well as the québécoised early exercise boundary* $\hat{b}$*, are given in the appendix.*

5 Numerical examples and discussion

Some numerical examples of vanilla, standard barrier and Parisian European and American option prices are given in Table 1. For simplicity, we consider a set of double-exponential jump-diffusion model specifications. The computed option prices are monotone functions of the volatility, the jump intensity, and the average positive and negative jump size (the reciprocals of the respective jump parameter values).

In Figure 2, we plot the European Parisian up-and-out put option (EPUOP) and the early exercise premium of the American Parisian up-and-out put option (APUOP EEP) as functions of the underlying asset price S_t and the Parisian window D in a double-exponential jump-diffusion model. First, we observe that both EPUOP and APUOP EEP are increasing functions of the underlying asset price and the Parisian window. Second, Parisian delta (gamma) is non-positive (non-negative). In the limiting case when the Parisian window is equal to zero (equal of greater than the option's time to maturity), Parisian option price, delta, and gamma converge to the values of their standard barrier (vanilla) counterparts. Hence, for $D = 0$, at $S_t = H$ Parisian delta is discontinuous and Parisian gamma diverges, whereas for $S_t > H$ both Parisian delta and gamma are equal to zero since options is knocked-out. Consequently, hedging of a standard barrier options is a difficult task because their Greeks are not well-behaved functions around the barrier level H. Parisian options are particularly attractive because Parisian delta and gamma are smooth functions of the underlying asset price, which is demonstrated in Panels C and D, E and F.

Table 1: Numerical examples. Prices of ATM and OTM vanilla, standard barrier, and Parisian European and American options in a double-exponential jump-diffusion model using the québécoisation method. The time to maturity is $\tau = 1$ year, and the Parisian window D is assumed to be either one week (1w) or one month (1m). The risk-free rate is $r = 0.05$, the dividend yield is $\delta = 0.01$, and the conditional probabilities of positive and negative jumps are $p = q = 0.5$.

Panel A: ATM options ($S_t = 100$, $K = 100$, $H = 110$).

Parameters				Vanilla		Barrier		Parisian (1w)		Parisian (1m)	
σ	λ	η	θ	Euro.	Amer.	Euro.	Amer.	Euro.	Amer.	Euro.	Amer.
0.2	1	25	25	6.23	6.54	4.70	4.99	5.20	5.50	5.66	5.96
0.2	1	25	50	6.13	6.43	4.66	4.95	5.14	5.44	5.59	5.89
0.2	1	50	25	6.12	6.44	4.62	4.92	5.11	5.42	5.57	5.88
0.2	1	50	50	6.02	6.33	4.58	4.88	5.06	5.36	5.49	5.80
0.2	5	25	25	7.30	7.59	5.25	5.54	5.86	6.15	6.47	6.76
0.2	5	25	50	6.83	7.11	5.09	5.36	5.64	5.92	6.16	6.44
0.2	5	50	25	6.80	7.12	4.91	5.21	5.49	5.80	6.05	6.37
0.2	5	50	50	6.31	6.62	4.72	5.02	5.24	5.54	5.72	6.02
0.3	1	25	25	9.93	10.22	5.91	6.18	7.12	7.40	8.25	8.54
0.3	1	25	50	9.86	10.15	5.90	6.16	7.09	7.37	8.21	8.50
0.3	1	50	25	9.85	10.14	5.87	6.14	7.07	7.35	8.20	8.48
0.3	1	50	50	9.78	10.07	5.85	6.12	7.04	7.32	8.15	8.44
0.3	5	25	25	10.69	10.98	6.19	6.46	7.50	7.77	8.76	9.04
0.3	5	25	50	10.36	10.64	6.12	6.38	7.38	7.64	8.57	8.85
0.3	5	50	25	10.33	10.62	6.00	6.26	7.26	7.54	8.48	8.77
0.3	5	50	50	9.98	10.27	5.92	6.18	7.14	7.41	8.29	8.57

Panel B: OTM options ($S_t = 105$, $K = 100$, $H = 110$).

Parameters				Vanilla		Barrier		Parisian (1w)		Parisian (1m)	
σ	λ	η	θ	Euro.	Amer.	Euro.	Amer.	Euro.	Amer.	Euro.	Amer.
0.2	1	25	25	4.55	4.74	2.29	2.42	2.97	3.13	3.61	3.79
0.2	1	25	50	4.45	4.64	2.26	2.40	2.93	3.09	3.56	3.73
0.2	1	50	25	4.45	4.65	2.23	2.37	2.90	3.06	3.53	3.72
0.2	1	50	50	4.35	4.54	2.21	2.34	2.86	3.02	3.48	3.65
0.2	5	25	25	5.58	5.78	2.66	2.79	3.48	3.64	4.29	4.47
0.2	5	25	50	5.11	5.29	2.56	2.69	3.32	3.47	4.04	4.21
0.2	5	50	25	5.12	5.33	2.41	2.55	3.18	3.35	3.93	4.13
0.2	5	50	50	4.63	4.82	2.30	2.44	3.00	3.16	3.66	3.84
0.3	1	25	25	8.16	8.37	2.98	3.11	4.44	4.61	5.85	6.04
0.3	1	25	50	8.09	8.30	2.97	3.10	4.42	4.59	5.81	6.00
0.3	1	50	25	8.09	8.30	2.95	3.08	4.40	4.57	5.79	5.99
0.3	1	50	50	8.01	8.22	2.94	3.07	4.38	4.55	5.76	5.95
0.3	5	25	25	8.91	9.13	3.17	3.30	4.75	4.92	6.30	6.49
0.3	5	25	50	8.58	8.78	3.13	3.26	4.66	4.82	6.14	6.32
0.3	5	50	25	8.56	8.78	3.02	3.15	4.55	4.72	6.05	6.24
0.3	5	50	50	8.21	8.42	2.98	3.11	4.46	4.62	5.88	6.07

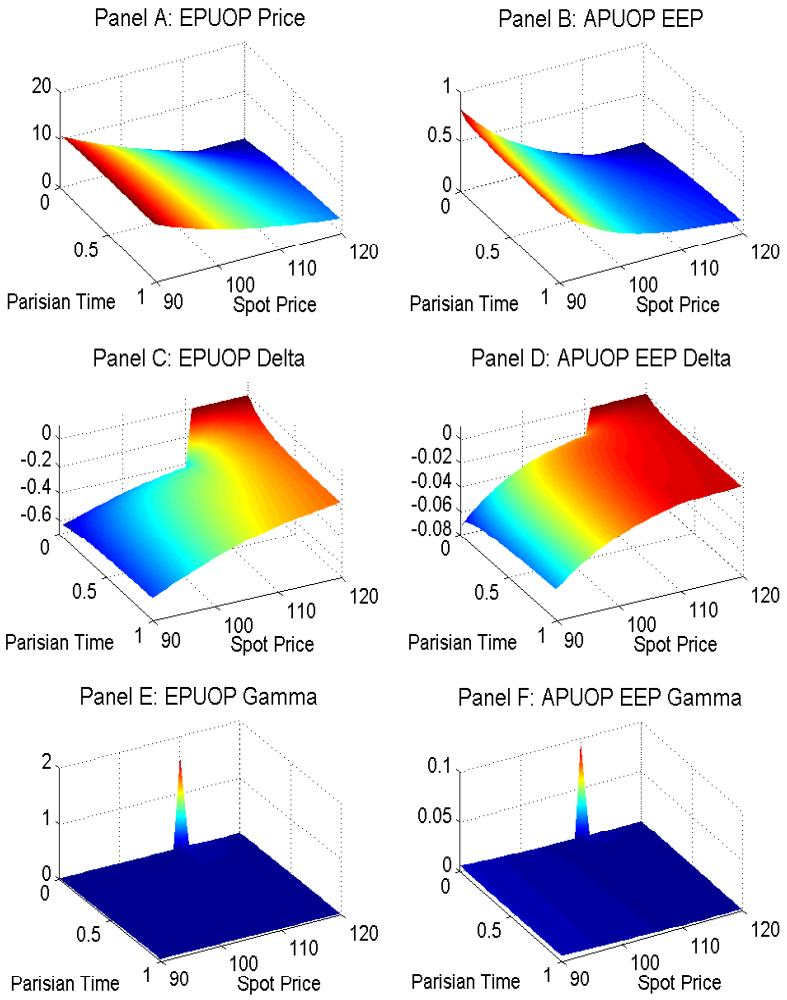

Figure 2: Prices and the Greeks (deltas and gammas) of European Parisian up-and-out put options (EPUOP) and early exercise premiums of American Parisian up-and-out put options (APOUP EEP) in a DEM model ($K = 100$, $H = 110$, $\tau = 1$ year, $r = 5\%$, $\delta = 1\%$, $\sigma = 20\%$, $p = q = 0.5$, $\lambda = 5$, $\eta = 50$, and $\theta = 25$) as a function of the underlying asset price $S_t \in [90, 120]$ and the Parisian window $D \in (0, 1)$.

6 Jump risk effects on Parisian options

In this section we investigate the effects of jumps on Parisian option prices and the Greeks. We again consider a double-exponential jump-diffusion model that is characterized with a diffusion parameter σ and a set of jump parameters $\{\lambda, p, \eta, \theta\}$. This model reduces to the Black-Scholes setting if the jump intensity is equal to zero ($\lambda = 0$). Since the vast

majority of the literature on the pricing of Parisian options is related to the Black-Scholes model, the inclusion of the jump risk in our paper naturally raises some questions about the effects of jumps on the Parisian option prices and the Greeks.

In Figure 3 we plot the dependence of the difference between Parisian option prices (and the corresponding deltas and gammas) with and without jumps on the underlying asset price S_t and the jump intensity λ. Other model parameters, i.e., p, η, and θ, are kept constant. Expectedly, the differences between prices, deltas, and gammas with and without jumps are vanishing as the jump intensity is approaching to zero. The EPUOP difference (Panel A) is always positive because the existence of (negative) jumps increases the probability of the option exercise. The APUOP EEP difference (Panel B) is always positive in the excursion and the standard continuation region. However, it becomes negative in the payoff exercise region. This is because the APUOP EEP is defined as the difference between the option's intrinsic value and the corresponding EPUOP price. Therefore, in the payoff exercise region, we observe an opposite behaviour of the APUOP EEP difference to that of the EPUOP difference presented in Panel A. The delta of an EPUOP option is negative, and therefore we conclude from Panel C that EPUOP is more sensitive to changes in the underlying asset price in a model with jumps than in the corresponding Black-Scholes setting. APUOP EEP delta difference, which is given in Panel D, follows a similar pattern as the APUOP EEP price difference discussed above. Finally, the effect of jumps on the Parisian gamma is relatively limited, as shown in Panels E and F. However, they exhibit the strongest impact at the barrier level H.

On the other hand, Figure 4 demonstrates the dependence of the difference between Parisian option prices (and the corresponding deltas and gammas) with and without jumps on the underlying asset price S_t and the negative jump parameter θ. Remaining jump parameters, i.e., p, λ, and η, are assumed to be constant. First, we observe that the EPUOP price difference is becoming more pronounced as the average size of negative jumps is increasing (Panel A). Similar conclusion holds for the APUOP EEP (Panel B), except in the payoff exercise region in the case when the expected size of negative jumps is very large. To explain this behavior, the line of argument developed for the APUOP EEP difference in Figure 3 can be adopted here as well. An increase in the average negative jump size leads to a higher sensitivity of the EPUOP price w.r.t. the underlying asset

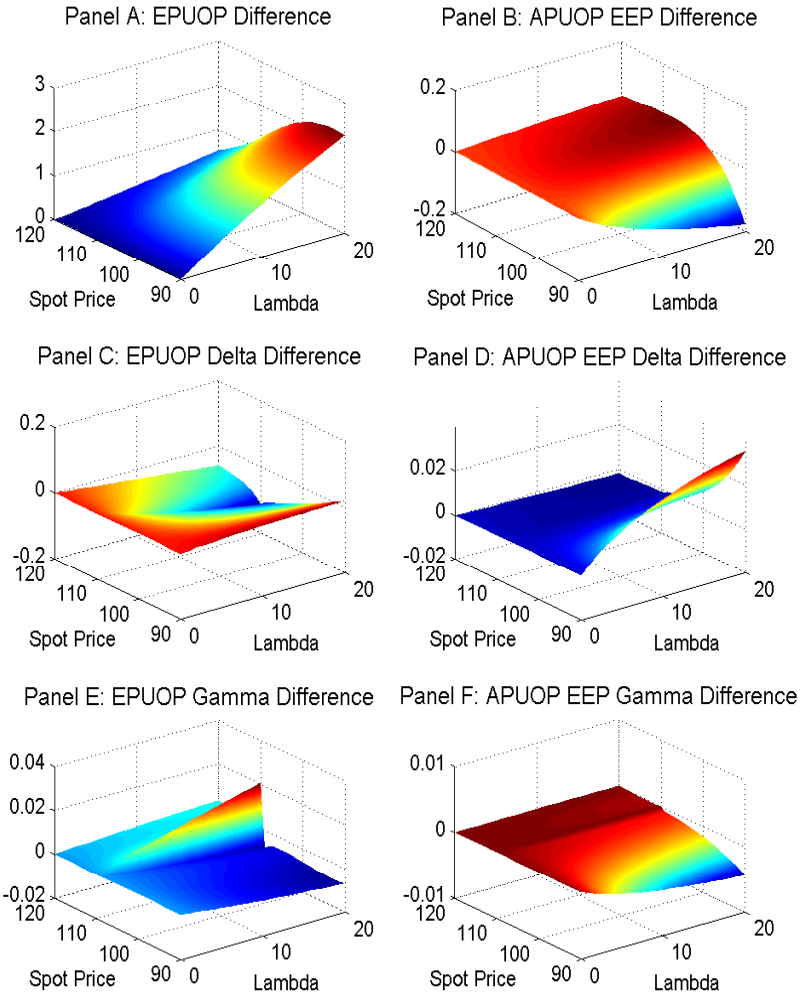

Figure 3: The differences between prices, deltas, and gammas of the European Parisian up-and-out put options (EPUOP) and the early exercise premiums of American Parisian up-and-out put options (APOUP EEP) with and without jumps, in a DEM model ($K = 100$, $H = 110$, $\tau = 1$ year, $r = 5\%$, $\delta = 1\%$, $\sigma = 20\%$, $p = q = 0.5$, $\eta = 50$, and $\theta = 25$) as functions of the underlying asset price $S_t \in [90, 120]$ and the jump intensity $\lambda \in [0, 20]$.

price (Panel B), as well as to an increase in the EPUOP gamma (Panel D), especially around the barrier level. Similarly, the APUOP EEP delta and gamma are elevated, although to much lesser extent, when negative jumps are more pronounced (Panels D and F). However, in the payoff exercise region, we observe the opposite effect.

Finally, we are interested in the dependence of EPUOP option price—for different lengths of Parisian window—on the (overall) risk-neutral drift μ, which is given in equation

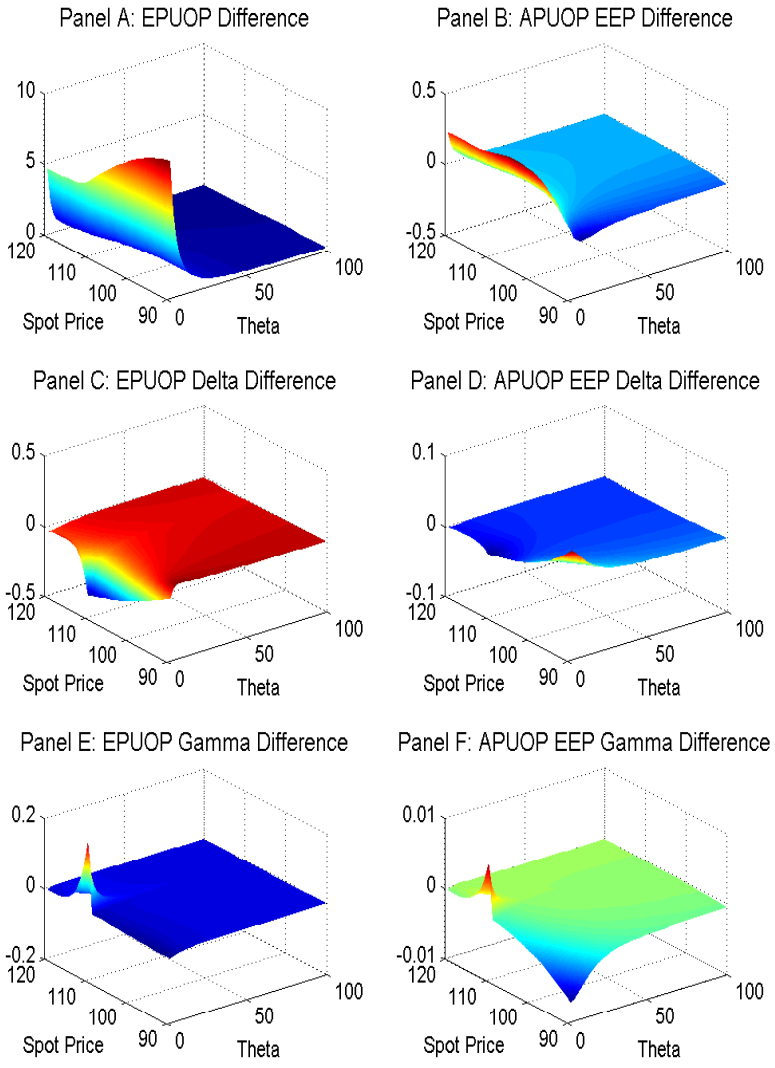

Figure 4: The differences between prices, deltas, and gammas of the European Parisian up-and-out put options (EPUOP) and the early exercise premiums of American Parisian up-and-out put options (APOUP EEP) with and without jumps, in a DEM model ($K = 100$, $H = 110$, $\tau = 1$ year, $r = 5\%$, $\delta = 1\%$, $\sigma = 20\%$, $\lambda = 5$, $p = q = 0.5$, and $\eta = 50$) as functions of the underlying asset price $S_t \in [90, 120]$ and the negative jump parameter $\theta \in [2, 100]$.

(4), and the volatility σ (or the jump intensity λ). Our numerical results are summarized in Figure 5. Although we consider only European Parisian up-and-out put options, similar conclusions can be derived for their American counterparts. Vanilla options are monotonically increasing functions of the volatility, i.e., the vega of a vanilla option is always non-negative. However, depending on the drift of the underlying process and

the volatility, European up-and-out standard barrier put options can exhibit a very different, i.e., a non-monotonic, behavior. In particular, we consider the case when the underlying asset price S_t is in the standard region and close to the barrier H, and the drift is non-positive. Our numerical experiments confirm that the vega of a standard up-and-out barrier option can be non-negative (non-positive) when the drift is close to zero (strongly negative). Consequently, there exists a range of "intermediate" negative drift values where vega changes its sign, i.e., the option price first increases with volatility until certain critical volatility level and then it decreases. This rather unusual pattern, which can be observed in Panel A in Figure 5, is attributed to the increasing probability of the knock-out event occurrence with the rising volatility. Similar results are obtained for European up-and-out standard barrier put option as a function of the jump intensity parameter and the risk-neutral drift (Panel B). More specifically, when the drift is close to zero (strongly negative), the option price sensitivity w.r.t. λ is non-negative (non-positive). Thus, similarly to the volatility case discussed above, there exists a range of negative drift values where the option price, as a function of the jump intensity, increases only until certain critical level is reached, after which it monotonically decreases.

It is worth mentioning that some interesting financial applications of the knock-out volatility effect for investment policy implications when the equity of a levered firm is modelled as a down-and-out call option are studied in Chesney and Gibson (1999, 2001) (in the Black-Scholes setting).

Existence of the volatility and jump intensity knock-out effects—the non-monotonic behavior of the option price w.r.t. the volatility and the jump intensity if the underlying process is closed to the knock-out barrier—is also expected in the case of Parisian options. By definition, standard barrier and vanilla options are two special cases of Parisian option contracts with the Parisian time being equal to zero and the option's time to maturity, respectively. Therefore, it is plausible to expect a similar knock-out effect for, at least, Parisian options with relatively short Parisian window D. To the best of our knowledge, this research question has not been addressed previously in the literature. Panels C and D in Figure 5 represents the EPUOP critical volatility and the critical jump intensity, respectively, as functions of the risk-neutral drift. In both cases we notice that the drift range(s) in which the EOUOP price exhibits the non-monotonic behavior, i.e., the region

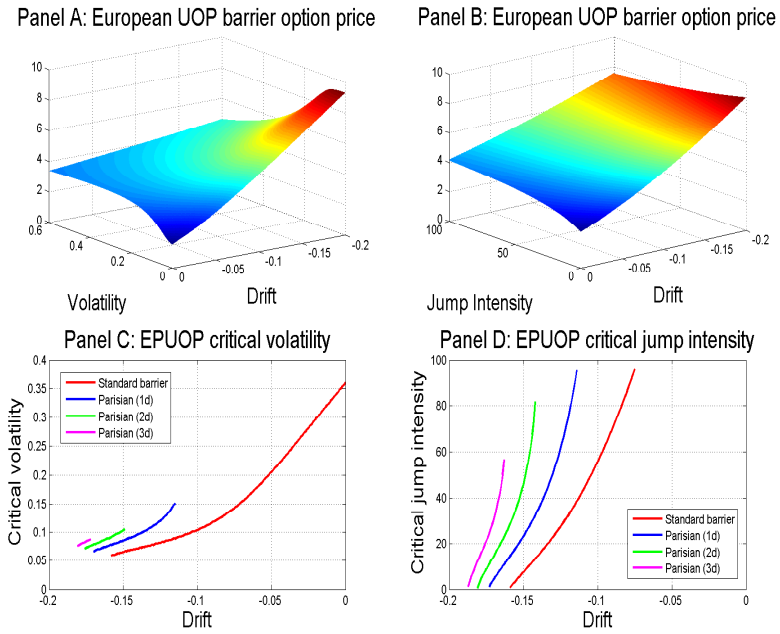

Figure 5: Knock-out volatility and jump intensity effects for European Parisian up-and-out put option as a function of the drift and either the volatility or the jump intensity in a DEM model ($S_t = K = 100$, $H = 105$, $\tau = 6$ months, $r = 2\%$, $p = q = 0.5$, $\lambda = 5$ (if fixed), and $\eta = \theta = 50$). If fixed, volatility and the jump intensity are $\sigma = 10\%$ and $\lambda = 5$, otherwise $\sigma \in (0, 0.4)$ and $\lambda \in (0, 100)$, respectively. The drift term is $\mu \in (-0.2, 0)$.

in which the critical volatility/jump intensity level exists, is shrinking with the increasing Parisian window. Moreover, for a given drift level in an overlapping "non-monotonic range"—e.g., in the Panel C (Panel D), for the drift in the range between -0.158 and -0.149 (between -0.159 and -0.142) there exist critical volatility (critical jump intensity) levels for EPUOP options with Parisian windows of 0, 1 and 2 days—the options with longer Parisian window have higher critical volatility/jump intensity. The observed pattern is consistent with the intuition that the probability of the knock-out event occurrence is inversely related to the length of the Parisian window. In the limiting case when Parisian window is larger or equal to the residual maturity, i.e., for vanilla options, the option price is monotonically increasing function of both volatility and jump intensity, and the critical knock-out behavior completely disappears. Therefore, our numerical findings are in line with theoretical expectations.

7 Conclusion

In this paper we study a new approach—québécoisation method—for the pricing of European and American Parisian options in a hyper-exponential jump-diffusion model. Following the idea of Zhu and Chen (2013), we first rotate the time coordinate system in the excursion region and reduce the dimensionality of our PIDE problem. We introduce a double Laplace-Carson transform w.r.t. the residual standard and excursion time, respectively, and obtain the transformed (québécoised) option prices and the Greeks (delta and gamma) in a closed form. In particular, we consider European and American Parisian up-and-out put options. Results for other types of Parisian options can be derived either by doing similar calculations or with the help of symmetry and/or parity relations that are discussed in the paper. The option prices and the Greeks in the original domain are computed using a two-dimensional Gaver-Stehfest inversion algorithm. Finally, we provide numerical examples for European and American up-and-out put option prices and the Greeks in a double-exponential jump-diffusion setting, and discuss the implications of the jump risk for Parisian options. To the best of our knowledge, American Parisian options are considered only in Haber, Schönbucher and Wilmott (1999) and Chesney and Gauthier (2006). On the other hand, the only paper that studies the pricing of Parisian options in a jump-diffusion framework is Albrecher, Kortschak and Zhou (2012), but they focus exclusively on European Parisian options and consider only double-exponential distribution of jump sizes. Therefore, our work contributes to the literature by developing a new method for pricing both European and American Parisian options in a very general and analytically tractable jump-diffusion framework.

References

Abate, J., W. Whitt. 2006. A unified framework for numerically inverting Laplace transforms. *INFORMS Journal on Computing* **18** 408–421.

Albrecher, H., D. Kortschak, X. Zhou. 2012. Pricing of Parisian options for a jump-diffusion model with two-sided jumps. *Applied Mathematical Finance* **19** 97–129.

Anderluh, J. H. M., J. A. M. van der Weide. 2009. Double-sided Parisian option pricing. *Finance and Stochastics* **13** 205–238.

Avellaneda, M., L. Wu. 1999. Pricing Parisian-style options with a lattice method. *International Journal of Theoretical and Applied Finance* **2** 1–16.

Avram, F., T. Chan, M. Usabel. 2002. On the valuation of constant barrier options under spectrally one-sided exponential Lévy models and Carr's approximation for American puts. *Stochastic Processes and their Applications* **100** 75–107.

Bernard, C., O. Le Courtois, F. Quitard-Pinon. 2005. A new procedure for pricing Parisian options. *The Journal of Derivatives* **12** 45–54.

Black, F., M. S. Scholes. 1973. The pricing of options and corporate liabilities. *Journal of Political Economy* **81** 637–654.

Cai, N. 2009. On first passage times of a hyper-exponential jump diffusion process. *Operations Research Letters* **37** 127–134.

Cai, N., N. Chen, X. Wan. 2010. Occupation times of jump-diffusion processes with double-exponential jumps and the pricing of options. *Mathematics of Operations Research* **35** 412–437.

Carr, P., R. Jarrow, R. Myneni. 1992. Alternative characterizations of American put options. *Mathematical Finance* **2** 87–106.

Carr, P. 1998. Randomization and the American put. *The Review of Financial Studies* **11** 597–626.

Chesney, M., M. Jeanblanc, M. Yor. 1997. Brownian excursions and Parisian barrier options. *Advances in Applied Probability* **29**, 165–184.

Chesney, M., J. Cornwall, M. Jeanblanc, G. Kentwall, M. Yor. 1997. Parisian pricing. Risk **10** 77–79.

Chesney, M., R. Gibson. 1999. The investment policy and the pricing of equity in a levered ÂŽfirm: A re-examination of the 'contingent claims' valuation approach. *The European Journal of Finance*. **5**, 95–107.

Chesney, M., R. Gibson. 2001. Reducing asset substitution with warrant and convertible debt issue. *The Journal of Derivatives*. **9**, 39–52.

Chesney, M., L. Gauthier. 2006. American Parisian options. *Finance and Stochastics*. **10** 475–506.

Choudhury, G. L., D. M. Lucantoni, W. Whitt. 1997. Numerical solution of piecewise-stationary $M_t/G_t/1$ queues. *Operations Research* **45** 451–463.

Cont, R., P. Tankov. 2004. Non-parametric calibration of jump-diffusion option pricing models. *Journal of Computational Finance* **7** 1–50.

Costabile, M. 2002. A combinatorial approach for pricing Parisian options. *Decisions in Economics and Finance* **25** 111–125.

Crosby, J., N. Le Saux, A. Mijatović. 2010. Approximating Lévy processes with a view to option prices. *International Journal of Theoretical and Applied Finance* **13** 63–91.

Detemple, J. 2005. American-style derivatives: Valuation and computation. CRC Press.

Fujita, T., R. Miura. 2002. Edokko options: A new framework for barrier options. *Asia-Pacific Financial Markets*. **9** 141–151.

Gao, B., J. Huang, M. Subrahmanyam. 2000. The valuation of American barrier options using the decomposition technique. *Journal of Economic Dynamics and Control* **24** 1783–1827.

Haber, R. J., P. J. Schönbucher, P. Wilmott. 1999. Pricing Parisian options. *The Journal of Derivatives* **6** 71–79.

Hugonnier, J. 1999. The Feynman-Kac formula and pricing occupation time derivatives. *International Journal of Theoretical and Applied Finance* **2** 153–178.

Jacka, S. D. 1991. Optimal stopping and the American put. *Mathematical Finance* **1** 1–14.

Jeanblanc, M., M. Yor, M. Chesney. 2009. Mathematical methods for financial markets. Springer.

Jeannin, M., M. Pistorius. 2010. A transform approach to compute prices and Greeks of barrier options driven by a class of Lévy processes. *Quantitative Finance* **10** 629–644.

Kim, I. J. 1990. The analytic valuation of American options. *Review of Financial Studies* **3** 547–572.

Kimura, T. 2010. Alternative randomization for valuing American options. *Asia-Pacific Journal of Operational Research* **27** 167–187.

Kou, S. G. 2002. A jump-diffusion model for option pricing. *Management Science* **48** 1086–1101.

Labart, C., J. Lelong. 2009. Pricing double Parisian options using Laplace tranforms. *International Journal of Theoretical and Applied Finance* **12** 19–44.

Lipton, A. 2002. Assets with jumps. *Risk* **15** 149–153.

Schröder, M. 2003. Brownian excursions and Parisian barrier options: A note. *Journal of Applied Probability* **40** 855–864.

Vetzal, K. R., P. A. Forsyth. 1999. Discrete Parisian and delayed barrier options: A general numerical approach. *Advances in Futures and Options Research* **10** 1–16 (1999)

Zhu, Z., N. Stokes. 1998. A finite element platform for pricing path dependent exotic options. CSIRO Working Paper.

Zhu, S.-P., W.-T. Chen. 2013. Pricing Parisian and *Parasian* options analytically. *Journal of Economic Dynamics and Control* **37** 875–896.

Appendix A Pricing of Québécoised European Parisian put options: Proof of Theorem 1

We start by introducing the change of variables, i.e., instead of the standard time t_s and the excursion time t_e we define $\tau_s := T - D - t_s$ and $\tau_e := D - t_e$, respectively. The PIDE system given in equation (30) becomes

$$\begin{cases} -\dfrac{\partial \tilde{\pi}_{uo}}{\partial \tau_e}(x,\tau_s,\tau_e) + \mathcal{L}\tilde{\pi}_{uo}(x,\tau_s,\tau_e) = r\tilde{\pi}_{uo}(x,\tau_s,\tau_e), & \text{if } (x,t_s,t_e) \in \tilde{\mathscr{E}}, \\ -\dfrac{\partial \tilde{\pi}_{uo}}{\partial \tau_s}(x,\tau_s,\tau_e) + \mathcal{L}\tilde{\pi}_{uo}(x,\tau_s,\tau_e) = r\tilde{\pi}_{uo}(x,t_s,t_e), & \text{if } (x,\tau_s,\tau_e) \in \tilde{\mathscr{S}}. \end{cases} \tag{66}$$

The notation in the equations (31)–(33) is adjusted accordingly. Applying the DLCT to our PIDE system results in two coupled OIDEs. In the standard region $\tilde{\mathscr{S}}$, the OIDE describing the dynamics of the québécoised Parisian up-and-out put option is

$$\begin{aligned} \frac{\sigma^2}{2}\frac{d^2\hat{\tilde{\pi}}_{uo}}{dx^2}(x,\alpha^s_{k_s},\alpha^e_{k_e}) + \mu\frac{d\hat{\tilde{\pi}}_{uo}}{dx}(x,\alpha^s_{k_s},\alpha^e_{k_e}) - (r+\alpha^s_{k_s}+\lambda)\hat{\tilde{\pi}}_{uo}(x,\alpha^s_{k_s},\alpha^e_{k_e}) \\ + \alpha^s_{k_s}p(x,D) + \lambda\int_{-\infty}^{+\infty}\hat{\tilde{\pi}}_{uo}(x+y,\alpha^s_{k_s},\alpha^e_{k_e})\varphi_Y(y)dy = 0, \end{aligned} \tag{67}$$

and in the excursion region $\tilde{\mathscr{E}}$ we have

$$\begin{aligned} \frac{\sigma^2}{2}\frac{d^2\hat{\tilde{\pi}}_{uo}}{dx^2}(x,\alpha^s_{k_s},\alpha^e_{k_e}) + \mu\frac{d\hat{\tilde{\pi}}_{uo}}{dx}(x,\alpha^s_{k_s},\alpha^e_{k_e}) - (r+\alpha^e_{k_e}+\lambda)\hat{\tilde{\pi}}_{uo}(x,\alpha^s_{k_s},\alpha^e_{k_e}) \\ + \lambda\int_{-\infty}^{+\infty}\hat{\tilde{\pi}}_{uo}(x+y,\alpha^s_{k_s},\alpha^e_{k_e})\varphi_Y(y)dy = 0. \end{aligned} \tag{68}$$

Québécoised initial conditions in the standard and the excursion region are absorbed in the system of OIDEs. On the other hand, the québécoised boundary condition in the standard region is

$$\lim_{x\downarrow-\infty}\hat{\tilde{\pi}}^s_{uo}(x,\alpha^s_{k_s}) = \frac{\alpha^s_{k_s}}{\alpha^s_{k_s}+r}\lim_{x\downarrow-\infty}p(x,D) = \frac{\alpha^s_{k_s}e^{\kappa}}{\alpha^s_{k_s}+r}, \tag{69}$$

and the québécoised boundary condition in the excursion region is given by

$$\lim_{x\uparrow+\infty}\hat{\tilde{\pi}}^e_{uo}(x,\alpha^e_{k_e}) = 0. \tag{70}$$

The transformed value-matching and smooth pasting conditions at the boundary between the corridor and the payoff subregions—which can be obtained from the third and the

fourth equation in (31)—are

$$\begin{aligned}\lim_{x\uparrow\kappa}\hat{\tilde{\pi}}^{s}_{uo}(x,\alpha^{s}_{k_s}) &= \lim_{x\downarrow\kappa}\hat{\tilde{\pi}}^{s}_{uo}(x,\alpha^{s}_{k_s}),\\ \lim_{x\uparrow\kappa}\frac{d\hat{\tilde{\pi}}^{s}_{uo}}{dx}(x,\alpha^{s}_{k_s}) &= \lim_{x\downarrow\kappa}\frac{d\hat{\tilde{\pi}}^{s}_{uo}}{dx}(x,\alpha^{s}_{k_s}),\end{aligned} \tag{71}$$

Finally, the québécoisation procedure transforms the high-contact conditions at the boundary between the standard and the excursion region to

$$\begin{aligned}\lim_{x\uparrow h}\hat{\tilde{\pi}}^{s}_{uo}(x,\alpha^{s}_{k_s}) &= \lim_{x\downarrow h}\hat{\tilde{\pi}}^{e}_{uo}(x,\alpha^{e}_{k_e}),\\ \lim_{x\uparrow h}\frac{d\hat{\tilde{\pi}}^{s}_{uo}}{dx}(x,\alpha^{s}_{k_s}) &= \lim_{x\downarrow h}\frac{d\hat{\tilde{\pi}}^{e}_{uo}}{dx}(x,\alpha^{e}_{k_e}).\end{aligned} \tag{72}$$

To solve the system of two-dimensional OIDEs we first consider the excursion region. Assuming the québécoised option price in the excursion region in the form (51), the two derivative terms in the OIDE (68) are

$$\begin{aligned}\frac{d\hat{\tilde{\pi}}^{e}_{uo}}{dx}(x,\alpha^{e}_{k_e}) &= \sum_{j=1}^{n+1} A^{-}_{j}\gamma_{j,r+\alpha^{e}_{k_e}}e^{\gamma_{j,r+\alpha^{e}_{k_e}}(x-h)},\\ \frac{d^2\hat{\tilde{\pi}}^{e}_{uo}}{dx^2}(x,\alpha^{e}_{k_e}) &= \sum_{j=1}^{n+1} A^{-}_{j}\gamma^{2}_{j,r+\alpha^{e}_{k_e}}e^{\gamma_{j,r+\alpha^{e}_{k_e}}(x-h)}.\end{aligned} \tag{73}$$

The integral term is defined as $\mathscr{I}(\tilde{\mathscr{E}}) := \int_{-\infty}^{+\infty}\hat{\tilde{\pi}}_{uo}(x+y,\alpha^{s}_{k_s},\alpha^{e}_{k_e})\varphi_Y(y)dy$, and it can be decomposed in the form

$$\mathscr{I}(\tilde{\mathscr{E}}) = \mathscr{I}(\tilde{\mathscr{E}}\big|\tilde{\mathscr{E}}^{+}) + \mathscr{I}(\tilde{\mathscr{E}}\big|\tilde{\mathscr{E}}^{-}) + \mathscr{I}(\tilde{\mathscr{E}}\big|\tilde{\mathscr{S}}_c) + \mathscr{I}(\tilde{\mathscr{E}}\big|\tilde{\mathscr{S}}_p). \tag{74}$$

The term $\mathscr{I}(\tilde{\mathscr{E}}\big|\tilde{\mathscr{E}}^{+})$ describes the positive jumps within the excursion region, and is given by

$$\mathscr{I}(\tilde{\mathscr{E}}\big|\tilde{\mathscr{E}}^{+}) = \int_{0}^{+\infty}\sum_{k=1}^{m}p_k\eta_k e^{-\eta_k y}\sum_{j=1}^{n+1}A^{-}_{j}e^{\gamma_{j,r+\alpha^{e}_{k_e}}(x+y-h)}dy, \tag{75}$$

and the term $\mathscr{I}(\tilde{\mathscr{E}}\big|\tilde{\mathscr{E}}^{-})$ describes the negative jumps within the excursion region, and it takes the form

$$\mathscr{I}(\tilde{\mathscr{E}}\big|\tilde{\mathscr{E}}^{-}) = \int_{h-x}^{0}\sum_{l=1}^{n}q_l\theta_l e^{\theta_l y}\sum_{j=1}^{n+1}A^{-}_{j}e^{\gamma_{j,r+\alpha^{e}_{k_e}}(x+y-h)}dy. \tag{76}$$

The (negative) jumps from the excursion region to the corridor region are captured by

the term $\mathscr{I}(\tilde{\mathscr{E}}|\tilde{\mathscr{S}}_c)$, which given by

$$\begin{aligned}\mathscr{I}(\tilde{\mathscr{E}}|\tilde{\mathscr{S}}_c) = &\int_{\kappa-x}^{h-x}\sum_{l=1}^{n} q_l\theta_l e^{\theta_l y}\left(\sum_{i=1}^{m+1} B_i^{+} e^{\beta_{i,r+\alpha^s_{k_s}}(x+y-h)} + \sum_{j=1}^{n+1} B_j^{-} e^{\gamma_{j,r+\alpha^s_{k_s}}(x+y-h)}\right) dy \\ &+ \int_{\kappa-x}^{h-x}\sum_{l=1}^{n} q_l\theta_l e^{\theta_l y}\sum_{k_v=1}^{2N}\varsigma_{k_v,N}\sum_{j=1}^{n+1}\overline{\omega}'_{j,k_v} e^{\gamma_{j,r+\alpha^v_{k_v}}(x+y-\kappa)} dy.\end{aligned} \tag{77}$$

Finally, the term $\mathscr{I}(\tilde{\mathscr{E}}|\tilde{\mathscr{S}}_p)$ quantifies the effect of the (negative) jumps from the excursion region to the payoff region, i.e.,

$$\begin{aligned}\mathscr{I}(\tilde{\mathscr{E}}|\tilde{\mathscr{S}}_p) = &\int_{-\infty}^{\kappa-x}\sum_{l=1}^{n} q_l\theta_l e^{\theta_l y}\sum_{k_v=1}^{2N}\varsigma_{k_v,N}\sum_{i=1}^{m+1}\underline{\omega}'_{i,k_v} e^{\beta_{i,r+\alpha^v_{k_v}}(x+y-\kappa)} dy \\ &+ \int_{-\infty}^{\kappa-x}\sum_{l=1}^{n} q_l\theta_l e^{\theta_l y}\sum_{k_v=1}^{2N}\varsigma_{k_v,N}\left(\frac{\alpha^s_{k_s}}{\alpha^s_{k_s}+r}\frac{\alpha^v_{k_v}}{\alpha^v_{k_v}+r}e^{\kappa} - \frac{\alpha^s_{k_s}}{\alpha^s_{k_s}+\delta}\frac{\alpha^v_{k_v}}{\alpha^v_{k_v}+\delta}e^{x+y}\right) dy.\end{aligned} \tag{78}$$

Therefore, after some algebra, the equation (68) becomes

$$\sum_{k=1}^{n+1} A_k^{-} e^{\gamma_{k,r+\alpha^e_{k_e}}(x-h)}\left(\Psi(\gamma_{k,r+\alpha^e_{k_e}}) - (\alpha^e_{k_e}+r)\right) + \sum_{l=1}^{n}\lambda q_l\theta_l e^{\theta_l(h-x)}\Phi_l(\tilde{\mathscr{E}}) = 0, \tag{79}$$

where $\Phi_l(\tilde{\mathscr{E}})$ $(l=1,2,...,n)$ is given by

$$\begin{aligned}\Phi_l(\tilde{\mathscr{E}}) := &\sum_{j=1}^{n+1}\frac{A_j^{-}}{\theta_l+\gamma_{j,r+\alpha^e_{k_e}}} - \sum_{i=1}^{m+1}\frac{B_i^{-}\left(1-e^{(\theta_l+\beta_{i,r+\alpha^s_{k_s}})(\kappa-h)}\right)}{\theta_l+\beta_{i,r+\alpha^s_{k_s}}} \\ &- \sum_{j=1}^{n+1}\frac{B_j^{-}\left(1-e^{(\theta_l+\gamma_{j,r+\alpha^s_{k_s}})(\kappa-h)}\right)}{\theta_l+\gamma_{j,r+\alpha^s_{k_s}}} - \sum_{i=1}^{m+1}\frac{C_i^{+}e^{\theta_l(\kappa-h)}}{\theta_l+\beta_{i,r+\alpha^s_{k_s}}} \\ &- \sum_{k_v=1}^{2N}\varsigma_{k_v,N}\sum_{i=1}^{m+1}\left(\frac{\underline{\omega}'_{i,k_v}e^{\theta_l(\kappa-h)}}{\theta_l+\beta_{i,r+\alpha^v_{k_v}}} + \sum_{j=1}^{n+1}\frac{\overline{\omega}'_{j,k_v}\left(e^{\gamma_{j,r+\alpha^v_{k_v}}(h-\kappa)} - e^{\theta_l(\kappa-h)}\right)}{\theta_l+\gamma_{j,r+\alpha^v_{k_v}}}\right) \\ &- \sum_{k_v=1}^{2N}\varsigma_{k_v,N}e^{\theta_l(\kappa-h)}\left(\frac{e^{\kappa}}{\theta_l}\frac{\alpha^s_{k_s}}{\alpha^s_{k_s}+r}\frac{\alpha^v_{k_v}}{\alpha^v_{k_v}+r} - \frac{e^{\kappa}}{\theta_l+1}\frac{\alpha^s_{k_s}}{\alpha^s_{k_s}+\delta}\frac{\alpha^v_{k_v}}{\alpha^v_{k_v}+\delta}\right).\end{aligned} \tag{80}$$

The first term on the l.h.s. of the equation (79) is equal to zero. For strictly positive jump intensity λ, the second term yields the set of conditions

$$\Phi_l(\tilde{\mathscr{E}}) = 0, \quad \text{for} \quad l=1,2,...,n. \tag{81}$$

Now we consider the corridor region $\tilde{\mathscr{S}}_c$. Assuming the québécoised option price in the form (52), the two derivative terms in the OIDE (67) are

$$\begin{aligned}
\frac{d\hat{\tilde{\pi}}^s_{uo}}{dx}(x,\alpha^s_{k_s}) &= \sum_{i=1}^{m+1}\beta_{i,r+\alpha^s_{k_s}}B_i^+ e^{\beta_{i,r+\alpha^s_{k_s}}(x-h)} + \sum_{j=1}^{n+1}\gamma_{j,r+\alpha^s_{k_s}}B_j^- e^{\gamma_{j,r+\alpha^s_{k_s}}(x-h)} \\
&\quad + \sum_{k_v=1}^{2N}\varsigma_{k_v,N}\sum_{j=1}^{n+1}\gamma_{j,r+\alpha^v_{k_v}}\overline{\omega}'_{j,k_v}e^{\gamma_{j,r+\alpha^v_{k_v}}(x-\kappa)}, \\
\frac{d^2\hat{\tilde{\pi}}^s_{uo}}{dx^2}(x,\alpha^s_{k_s}) &= \sum_{i=1}^{m+1}\beta^2_{i,r+\alpha^s_{k_s}}B_i^+ e^{\beta_{i,r+\alpha^s_{k_s}}(x-h)} + \sum_{j=1}^{n+1}\gamma^2_{j,r+\alpha^s_{k_s}}B_j^- e^{\gamma_{j,r+\alpha^s_{k_s}}(x-h)} \\
&\quad + \sum_{k_v=1}^{2N}\varsigma_{k_v,N}\sum_{j=1}^{n+1}\gamma^2_{j,r+\alpha^v_{k_v}}\overline{\omega}'_{j,k_v}e^{\gamma_{j,r+\alpha^v_{k_v}}(x-\kappa)}.
\end{aligned} \tag{82}$$

The integral term in the equation (67), defined as $\mathscr{I}(\tilde{\mathscr{S}}_c) := \int_{-\infty}^{+\infty}\hat{\tilde{\pi}}_{uo}(x+y,\alpha^s_{k_s},\alpha^e_{k_e})\varphi_Y(y)dy$ can be decomposed as

$$\mathscr{I}(\tilde{\mathscr{S}}_c) = \mathscr{I}(\tilde{\mathscr{S}}_c|\tilde{\mathscr{E}}) + \mathscr{I}(\tilde{\mathscr{S}}_c|\tilde{\mathscr{S}}_c^+) + \mathscr{I}(\tilde{\mathscr{S}}_c|\tilde{\mathscr{S}}_c^-) + \mathscr{I}(\tilde{\mathscr{S}}_c|\tilde{\mathscr{S}}_p). \tag{83}$$

The term $\mathscr{I}(\tilde{\mathscr{S}}_c|\tilde{\mathscr{E}})$ describes the effect of the (positive) jumps from the corridor region to the excursion region:

$$\mathscr{I}(\tilde{\mathscr{S}}_c|\tilde{\mathscr{E}}) = \int_{h-x}^{+\infty}\sum_{k=1}^{m}p_k\eta_k e^{-\eta_k y}\sum_{j=1}^{n+1}A_j^- e^{\gamma_{j,r+\alpha^e_{k_e}}(x+y-h)}dy. \tag{84}$$

The terms $\mathscr{I}(\tilde{\mathscr{S}}_c|\tilde{\mathscr{S}}_c^+)$ and $\mathscr{I}(\tilde{\mathscr{S}}_c|\tilde{\mathscr{S}}_c^-)$ capture the positive and negative jumps within the corridor region, respectively, and they are given as follows

$$\begin{aligned}
\mathscr{I}(\tilde{\mathscr{S}}_c|\tilde{\mathscr{S}}_c^+) &= \int_0^{h-x}\sum_{k=1}^{m}p_k\eta_k e^{-\eta_k y}\left(\sum_{i=1}^{m+1}B_i^+ e^{\beta_{i,r+\alpha^s_{k_s}}(x+y-h)} + \sum_{j=1}^{n+1}B_j^- e^{\gamma_{j,r+\alpha^s_{k_s}}(x+y-h)}\right)dy \\
&\quad + \int_0^{h-x}\sum_{k=1}^{m}p_k\eta_k e^{-\eta_k y}\sum_{k_v=1}^{2N}\varsigma_{k_v,N}\sum_{j=1}^{n+1}\overline{\omega}'_{j,k_v}e^{\gamma_{j,r+\alpha^v_{k_v}}(x+y-\kappa)}dy,
\end{aligned} \tag{85}$$

and

$$\mathscr{I}(\tilde{\mathscr{S}}_c\big|\tilde{\mathscr{S}}_c^-) = \int_{\kappa-x}^{0}\sum_{l=1}^{n} q_l\theta_l e^{\theta_l y}\left(\sum_{i=1}^{m+1} B_i^+ e^{\beta_{i,r+\alpha_{k_s}^s}(x+y-h)} + \sum_{j=1}^{n+1} B_j^- e^{\gamma_{j,r+\alpha_{k_s}^s}(x+y-h)}\right)dy$$
$$+ \int_{\kappa-x}^{0}\sum_{l=1}^{n} q_l\theta_l e^{\theta_l y}\sum_{k_v=1}^{2N}\varsigma_{k_v,N}\sum_{j=1}^{n+1}\overline{\omega}'_{j,k_v} e^{\gamma_{j,r+\alpha_{k_v}^v}(x+y-\kappa)}dy. \tag{86}$$

The term that captures the (negative) jumps from the corridor region to the payoff region is denoted by $\mathscr{I}(\tilde{\mathscr{S}}_c\big|\tilde{\mathscr{S}}_p)$, and it can be computed as

$$\mathscr{I}(\tilde{\mathscr{S}}_c\big|\tilde{\mathscr{S}}_p) = \int_{-\infty}^{\kappa-x}\sum_{l=1}^{n} q_l\theta_l e^{\theta_l y}\sum_{k_v=1}^{2N}\varsigma_{k_v,N}\sum_{i=1}^{m+1}\underline{\omega}'_{i,k_v} e^{\beta_{i,r+\alpha_{k_v}^v}(x+y-\kappa)}dy$$
$$+ \int_{-\infty}^{\kappa-x}\sum_{l=1}^{n} q_l\theta_l e^{\theta_l y}\sum_{k_v=1}^{2N}\varsigma_{k_v,N}\left(\frac{\alpha_{k_s}^s}{\alpha_{k_s}^s+r}\frac{\alpha_{k_v}^v}{\alpha_{k_v}^v+r}e^{\kappa} - \frac{\alpha_{k_s}^s}{\alpha_{k_s}^s+\delta}\frac{\alpha_{k_v}^v}{\alpha_{k_v}^v+\delta}e^{x+y}\right)dy. \tag{87}$$

Plugging the results for the two derivative terms and the jump integral back to (67), we obtain the equation

$$\begin{aligned}
&\sum_{k=1}^{m+1} B_k^+ e^{\beta_{k,r+\alpha_{k_s}^s}(x-h)}\left(\Psi(\beta_{k,r+\alpha_{k_s}^s}) - (\alpha_{k_s}^s+r)\right)\\
&+\sum_{l=1}^{n+1} B_l^- e^{\gamma_{l,r+\alpha_{k_s}^s}(x-h)}\left(\Psi(\gamma_{l,r+\alpha_{k_s}^s}) - (\alpha_{k_s}^s+r)\right)\\
&+\sum_{k_v=1}^{2N}\varsigma_{k_v,N}\sum_{l=1}^{n+1}\overline{\omega}'_{l,k_v} e^{\gamma_{l,r+\alpha_{k_v}^v}(x-\kappa)}\left(\Psi(\gamma_{l,r+\alpha_{k_v}^v}) - (\alpha_{k_v}^v+r)\right)\\
&+\sum_{k_v=1}^{2N}\varsigma_{k_v,N}\sum_{l=1}^{n+1} e^{\gamma_{l,r+\alpha_{k_v}^v}(x-\kappa)}\left(\alpha_{k_s}^s\overline{\omega}_{l,k_v} - (\alpha_{k_s}^s-\alpha_{k_v}^v)\overline{\omega}'_{l,k_v}\right)\\
&+\sum_{k=1}^{m}\lambda p_k\eta_k e^{\eta_k(x-h)}\Xi_k(\tilde{\mathscr{S}}_c) + \sum_{l=1}^{n}\lambda q_l\theta_l e^{\theta_l(h-x)}\Phi_l(\tilde{\mathscr{S}}_c) = 0,
\end{aligned} \tag{88}$$

where for all $k = 1, 2, ..., m$:

$$\begin{aligned}
\Xi_k(\tilde{\mathscr{S}}_c) := &\sum_{j=1}^{n+1}\frac{A_j^-}{\eta_k - \gamma_{j,r+\alpha_{k_e}^e}} - \sum_{i=1}^{m+1}\frac{B_i^+}{\eta_k - \beta_{i,r+\alpha_{k_s}^s}} - \sum_{j=1}^{n+1}\frac{B_j^-}{\eta_k - \gamma_{j,r+\alpha_{k_s}^s}}\\
&- \sum_{k_v=1}^{2N}\varsigma_{k_v,N}\sum_{j=1}^{n+1}\frac{\overline{\omega}'_{j,k_v} e^{\gamma_{j,r+\alpha_{k_s}^s}(h-\kappa)}}{\eta_k - \gamma_{j,r+\alpha_{k_v}^v}},
\end{aligned} \tag{89}$$

and for $l = 1, 2, ..., n$:

$$\begin{aligned}\Phi_l(\tilde{\mathscr{S}_c}) := &\sum_{i=1}^{m+1} \frac{B_i^+ e^{\beta_{i,r+\alpha_{k_s}^s}(\kappa-h)}}{\theta_l + \beta_{i,r+\alpha_{k_s}^s}} + \sum_{j=1}^{n+1} \frac{B_j^- e^{\gamma_{j,r+\alpha_{k_s}^s}(\kappa-h)}}{\theta_l + \gamma_{j,r+\alpha_{k_s}^s}} - \sum_{i=1}^{m+1} \frac{C_i^+}{\theta_l + \beta_{i,r+\alpha_{k_s}^s}} \\ &- \sum_{k_v=1}^{2N} \varsigma_{k_v,N} \left(\sum_{i=1}^{m+1} \frac{\underline{\omega}'_{i,k_v}}{\theta_l + \beta_{i,r+\alpha_{k_v}^v}} - \sum_{j=1}^{n+1} \frac{\overline{\omega}'_{j,k_v}}{\theta_l + \gamma_{j,r+\alpha_{k_v}^v}} \right) \\ &- \sum_{k_v=1}^{2N} \varsigma_{k_v,N} \left(\frac{e^\kappa}{\theta_l} \frac{\alpha_{k_s}^s}{\alpha_{k_s}^s + r} \frac{\alpha_{k_v}^v}{\alpha_{k_v}^v + r} - \frac{e^\kappa}{\theta_l + 1} \frac{\alpha_{k_s}^s}{\alpha_{k_s}^s + \delta} \frac{\alpha_{k_v}^v}{\alpha_{k_v}^v + \delta} \right).\end{aligned} \tag{90}$$

The equation (88) is satisfied if the following conditions hold

$$\begin{cases} \Xi_k(\tilde{\mathscr{S}_c}) = 0, & \text{for } \; k = 1, 2, ..., m, \\ \Phi_l(\tilde{\mathscr{S}_c}) = 0, & \text{for } \; l = 1, 2, ..., n, \end{cases} \tag{91}$$

and also if it holds that

$$\overline{\omega}'_{l,k_v} = \frac{\alpha_{k_s}^s \overline{\omega}_{l,k_v}}{\alpha_{k_s}^s - \alpha_{k_v}^v}, \quad \text{for } \; l = 1, ..., n \;\; \text{and} \;\; k_v = 1, ..., 2N. \tag{92}$$

Finally, we analyze the solution in the payoff region $\tilde{\mathscr{S}_p}$. Using the ansatz (53) we first compute the derivative terms

$$\begin{aligned}\frac{d\hat{\tilde{\pi}}_{uo}^s}{dx}(x, \alpha_{k_s}^s) = &\sum_{i=1}^{m+1} \beta_{i,r+\alpha_{k_s}^s} C_i^+ e^{\beta_{i,r+\alpha_{k_s}^s}(x-\kappa)} \\ &+ \sum_{k_v=1}^{2N} \varsigma_{k_v,N} \left(\sum_{i=1}^{m+1} \beta_{i,r+\alpha_{k_v}^v} \underline{\omega}'_{i,k_v} e^{\beta_{i,r+\alpha_{k_v}^v}(x-\kappa)} - \frac{\alpha_{k_s}^s}{\alpha_{k_s}^s + \delta} \frac{\alpha_{k_v}^v}{\alpha_{k_v}^v + \delta} e^x \right), \\ \frac{d^2\hat{\tilde{\pi}}_{uo}^s}{dx^2}(x, \alpha_{k_s}^s) = &\sum_{i=1}^{m+1} \beta_{i,r+\alpha_{k_s}^s}^2 C_i^+ e^{\beta_{i,r+\alpha_{k_s}^s}(x-\kappa)} \\ &+ \sum_{k_v=1}^{2N} \varsigma_{k_v,N} \left(\sum_{i=1}^{m+1} \beta_{i,r+\alpha_{k_v}^v}^2 \underline{\omega}'_{i,k_v} e^{\beta_{i,r+\alpha_{k_v}^v}(x-\kappa)} - \frac{\alpha_{k_s}^s}{\alpha_{k_s}^s + \delta} \frac{\alpha_{k_v}^v}{\alpha_{k_v}^v + \delta} e^x \right).\end{aligned} \tag{93}$$

The integral term in the standard payoff region, i.e., $\mathscr{I}(\tilde{\mathscr{S}_p}) := \int_{-\infty}^{+\infty} \hat{\tilde{\pi}}_{uo}(x+y, \alpha_{k_s}^s, \alpha_{k_e}^e) \varphi_Y(y) dy$, can be decomposed as

$$\mathscr{I}(\tilde{\mathscr{S}_p}) = \mathscr{I}(\tilde{\mathscr{S}_p} | \tilde{\mathscr{E}}) + \mathscr{I}(\tilde{\mathscr{S}_p} | \tilde{\mathscr{S}_c}) + \mathscr{I}(\tilde{\mathscr{S}_p} | \tilde{\mathscr{S}_p^+}) + \mathscr{I}(\tilde{\mathscr{S}_p} | \tilde{\mathscr{S}_p^-}). \tag{94}$$

The term $\mathscr{I}(\tilde{\mathscr{S}_p} | \tilde{\mathscr{E}})$ describes the effect of the (positive) jumps from the payoff region to

the excursion region, and is given by

$$\mathscr{I}(\tilde{\mathscr{S}}_p\big|\tilde{\mathscr{E}}) = \int_{h-x}^{+\infty} \sum_{k=1}^{m} p_k \eta_k e^{-\eta_k y} \sum_{j=1}^{n+1} A_j^- e^{\gamma_{j,r+\alpha_{k_e}^e}(x+y-h)} dy. \tag{95}$$

The effect of the (positive) jumps from the payoff region to the corridor region is captured by the term $\mathscr{I}(\tilde{\mathscr{S}}_p\big|\tilde{\mathscr{S}}_c)$, which is given in the form

$$\begin{aligned}\mathscr{I}(\tilde{\mathscr{S}}_p\big|\tilde{\mathscr{S}}_c) = &\int_{\kappa-x}^{h-x} \sum_{k=1}^{m} p_k \eta_k e^{-\eta_k y} \left(\sum_{i=1}^{m+1} B_i^+ e^{\beta_{i,r+\alpha_{k_s}^s}(x+y-h)} + \sum_{j=1}^{n+1} B_j^- e^{\gamma_{j,r+\alpha_{k_s}^s}(x+y-h)} \right) dy \\ &+ \int_{\kappa-x}^{h-x} \sum_{k=1}^{m} p_k \eta_k e^{-\eta_k y} \sum_{k_v=1}^{2N} \varsigma_{k_v,N} \sum_{j=1}^{n+1} \overline{\omega}'_{j,k_v} e^{\gamma_{j,r+\alpha_{k_v}^v}(x+y-\kappa)} dy.\end{aligned} \tag{96}$$

Finally, $\mathscr{I}(\tilde{\mathscr{S}}_p\big|\tilde{\mathscr{S}}_p^+)$ and $\mathscr{I}(\tilde{\mathscr{S}}_p\big|\tilde{\mathscr{S}}_p^-)$ are related to the positive and negative jumps, respectively, within the payoff region:

$$\begin{aligned}\mathscr{I}(\tilde{\mathscr{S}}_p\big|\tilde{\mathscr{S}}_p^+) = &\int_0^{\kappa-x} \sum_{k=1}^{m} p_k \eta_k e^{-\eta_k y} \sum_{k_v=1}^{2N} \varsigma_{k_v,N} \sum_{i=1}^{m+1} \underline{\omega}'_{i,k_v} e^{\beta_{i,r+\alpha_{k_v}^v}(x+y-\kappa)} dy \\ &+ \int_0^{\kappa-x} \sum_{k=1}^{m} p_k \eta_k e^{-\eta_k y} \sum_{k_v=1}^{2N} \varsigma_{k_v,N} \left(\frac{\alpha_{k_s}^s}{\alpha_{k_s}^s + r} \frac{\alpha_{k_v}^v}{\alpha_{k_v}^v + r} e^{\kappa} - \frac{\alpha_{k_s}^s}{\alpha_{k_s}^s + \delta} \frac{\alpha_{k_v}^v}{\alpha_{k_v}^v + \delta} e^{x+y} \right) dy,\end{aligned} \tag{97}$$

and

$$\begin{aligned}\mathscr{I}(\tilde{\mathscr{S}}_p\big|\tilde{\mathscr{S}}_p^-) = &\int_{-\infty}^{0} \sum_{l=1}^{n} q_l \theta_l e^{\theta_l y} \sum_{i=1}^{m+1} C_i^+ e^{\beta_{i,r+\alpha_{k_s}^s}(x+y-\kappa)} dy \\ &+ \int_{-\infty}^{0} \sum_{l=1}^{n} q_l \theta_l e^{\theta_l y} \sum_{k_v=1}^{2N} \varsigma_{k_v,N} \sum_{i=1}^{m+1} \underline{\omega}'_{i,k_v} e^{\beta_{i,r+\alpha_{k_v}^v}(x+y-\kappa)} dy \\ &+ \int_{-\infty}^{0} \sum_{l=1}^{n} q_l \theta_l e^{\theta_l y} \sum_{k_v=1}^{2N} \varsigma_{k_v,N} \left(\frac{\alpha_{k_s}^s}{\alpha_{k_s}^s + r} \frac{\alpha_{k_v}^v}{\alpha_{k_v}^v + r} e^{\kappa} - \frac{\alpha_{k_s}^s}{\alpha_{k_s}^s + \delta} \frac{\alpha_{k_v}^v}{\alpha_{k_v}^v + \delta} e^{x+y} \right) dy.\end{aligned} \tag{98}$$

After some algebra, we obtain the following equation

$$\begin{aligned}
&\sum_{k=1}^{m+1} C_k^+ e^{\beta_{k,r+\alpha_{k_s}^s}(x-\kappa)} \left(\Psi(\beta_{k,r+\alpha_{k_s}^s}) - (\alpha_{k_s}^s + r)\right) \\
&+ \sum_{k_v=1}^{2N} \varsigma_{k_v,N} \sum_{k=1}^{m+1} \underline{\omega}'_{k,k_v} e^{\beta_{k,r+\alpha_{k_v}^v}(x-\kappa)} \left(\Psi(\beta_{k,r+\alpha_{k_v}^v}) - (\alpha_{k_v}^v + r)\right) \\
&+ \sum_{k_v=1}^{2N} \varsigma_{k_v,N} \sum_{k=1}^{m+1} e^{\beta_{k,r+\alpha_{k_v}^v}(x-\kappa)} \left(\alpha_{k_s}^s \underline{\omega}_{k,k_v} - (\alpha_{k_s}^s - \alpha_{k_v}^v)\underline{\omega}'_{k,k_v}\right) \\
&+ \sum_{k=1}^{m} \lambda p_k \eta_k e^{\eta_k(x-h)} \Xi_k(\tilde{\mathscr{S}}_p) = 0,
\end{aligned} \tag{99}$$

where the coefficients $\Xi_k(\tilde{\mathscr{S}}_p)$ are defined for all $k = 1, 2, ..., m$ as

$$\begin{aligned}
\Xi_k(\tilde{\mathscr{S}}_p) :=& \sum_{j=1}^{n+1} \frac{A_j^-}{\eta_k - \gamma_{j,r+\alpha_{k_e}^e}} - \sum_{i=1}^{m+1} \frac{B_i^+ \left(1 - e^{(\eta_k - \beta_{i,r+\alpha_{k_s}^s})(h-\kappa)}\right)}{\eta_k - \beta_{i,r+\alpha_{k_s}^s}} \\
&- \sum_{j=1}^{n+1} \frac{B_j^- \left(1 - e^{(\eta_k - \gamma_{j,r+\alpha_{k_s}^s})(h-\kappa)}\right)}{\eta_k - \gamma_{j,r+\alpha_{k_s}^s}} - \sum_{i=1}^{m+1} \frac{C_i^+ e^{\eta_k(h-\kappa)}}{\eta_k - \beta_{i,r+\alpha_{k_s}^s}} \\
&- \sum_{k_v=1}^{2N} \varsigma_{k_v,N} \left(\sum_{i=1}^{m+1} \frac{\underline{\omega}'_{i,k_v} e^{\eta_k(h-\kappa)}}{\eta_k - \beta_{i,r+\alpha_{k_v}^v}} - \sum_{j=1}^{n+1} \frac{\overline{\omega}'_{j,k_v} \left(e^{\eta_k(h-\kappa)} - e^{\gamma_{j,r+\alpha_{k_v}^v}(h-\kappa)}\right)}{\eta_k - \gamma_{j,r+\alpha_{k_v}^v}} \right) \\
&- \sum_{k_v=1}^{2N} \varsigma_{k_v,N} e^{\eta_k(h-\kappa)} \left(\frac{e^\kappa}{\eta_k} \frac{\alpha_{k_s}^s}{\alpha_{k_s}^s + r} \frac{\alpha_{k_v}^v}{\alpha_{k_v}^v + r} - \frac{e^\kappa}{\eta_k - 1} \frac{\alpha_{k_s}^s}{\alpha_{k_s}^s + \delta} \frac{\alpha_{k_v}^v}{\alpha_{k_v}^v + \delta} \right).
\end{aligned} \tag{100}$$

The equation (99) is satisfied if

$$\Xi_k(\tilde{\mathscr{S}}_p) = 0, \quad \text{for} \quad k = 1, 2, ..., m. \tag{101}$$

In addition, the following condition has to hold

$$\underline{\omega}'_{k,k_v} = \frac{\alpha_{k_s}^s \underline{\omega}_{k,k_v}}{\alpha_{k_s}^s - \alpha_{k_v}^v}, \quad \text{for} \quad k = 1, ..., m \quad \text{and} \quad k_v = 1, ..., 2N. \tag{102}$$

The value matching and the smooth pasting conditions at $x = h$ are, respectively,

$$\begin{aligned}
\sum_{j=1}^{n+1} A_j^- - \sum_{i=1}^{m+1} B_i^+ - \sum_{j=1}^{n+1} B_j^- &= \sum_{k_v=1}^{2N} \varsigma_{k_v,N} \sum_{j=1}^{n+1} \overline{w}'_{j,k} e^{\gamma_{j,r+\alpha^v_{k_v}}(h-\kappa)}, \\
\sum_{j=1}^{n+1} \gamma_{j,r+\alpha^e_{k_e}} A_j^- - \sum_{i=1}^{m+1} \beta_{i,r+\alpha^s_{k_s}} B_i^+ - \sum_{j=1}^{n+1} \gamma_{j,r+\alpha^s_{k_s}} B_j^- &= \sum_{k_v=1}^{2N} \varsigma_{k_v,N} \sum_{j=1}^{n+1} \gamma_{j,r+\alpha^v_{k_v}} \overline{\omega}'_{j,k_v} e^{\gamma_{j,r+\alpha^v_{k_v}}(h-\kappa)},
\end{aligned} \tag{103}$$

whereas at $x = \kappa$ we obtain the conditions

$$\begin{aligned}
&\sum_{i=1}^{m+1} B_i^+ e^{\beta_{i,r+\alpha^s_{k_s}}(\kappa-h)} + \sum_{j=1}^{n+1} B_j^+ e^{\gamma_{j,r+\alpha^s_{k_s}}(\kappa-h)} - \sum_{i=1}^{m+1} C_i^+ \\
&= \sum_{k_v=1}^{2N} \varsigma_{k_v,N} \left(\sum_{i=1}^{m+1} \underline{\omega}'_{i,k_v} - \sum_{j=1}^{n+1} \overline{\omega}'_{j,k_v} + \left(\frac{\alpha^s_{k_s}}{\alpha^s_{k_s}+r} \frac{\alpha^v_{k_v}}{\alpha^v_{k_v}+r} e^{\kappa} - \frac{\alpha^s_{k_s}}{\alpha^s_{k_s}+\delta} \frac{\alpha^v_{k_v}}{\alpha^v_{k_v}+\delta} e^{\kappa} \right) \right), \\
&\sum_{i=1}^{m+1} \beta_{i,r+\alpha^s_{k_s}} B_i^+ e^{\beta_{i,r+\alpha^s_{k_s}}(\kappa-h)} + \sum_{j=1}^{n+1} \gamma_{j,r+\alpha^s_{k_s}} B_j^+ e^{\gamma_{j,r+\alpha^s_{k_s}}(\kappa-h)} - \sum_{i=1}^{m+1} \beta_{i,r+\alpha^s_{k_s}} C_i^+ \\
&= \sum_{k_v=1}^{2N} \varsigma_{k_v,N} \left(\sum_{i=1}^{m+1} \beta_{i,r+\alpha^v_{k_v}} \underline{\omega}'_{i,k_v} - \sum_{j=1}^{n+1} \gamma_{j,r+\alpha^v_{k_v}} \overline{\omega}'_{j,k_v} - \frac{\alpha^s_{k_s}}{\alpha^s_{k_s}+\delta} \frac{\alpha^v_{k_v}}{\alpha^v_{k_v}+\delta} e^{\kappa} \right).
\end{aligned} \tag{104}$$

The unknown coefficients solve the system of linear equations

$$\mathbf{P}\mathbf{u}_e = \mathbf{p}_e, \tag{105}$$

where $\mathbf{u}_e := (\mathbf{a}^-, \mathbf{b}^+, \mathbf{b}^-, \mathbf{c}^+)'$, with the elements are defined as $\mathbf{a}^- := (A_1^-, ..., A_{n+1}^-)'$, $\mathbf{b}^+ := (B_1^+, ..., B_{m+1}^+)'$, $\mathbf{b}^- := (B_1^-, ..., B_{n+1}^-)'$, and $\mathbf{c}^+ := (C_1^+, ..., C_{m+1}^+)'$. The vector $\mathbf{p}_e := (\mathbf{p}_{e,1}, \mathbf{p}_{e,2}, \mathbf{p}_{e,3}, \mathbf{p}_{e,4}, \mathbf{p}_{e,5}, \mathbf{p}_{e,6}, \mathbf{p}_{e,7}, \mathbf{p}_{e,8})'$ is a $(2n + 2m + 4)$-dimensional column vector.

The elements $\mathbf{p}_{e,1}, \mathbf{p}_{e,2}, \mathbf{p}_{e,4}, \mathbf{p}_{e,5} \in \mathbb{R}^{1\times 1}$ are given by

$$
\begin{aligned}
\mathbf{p}_{e,1} &= \sum_{k_v=1}^{2N} \varsigma_{k_v,N} \sum_{j=1}^{n+1} \overline{w}'_{j,k_v} e^{\gamma_{j,r+\alpha^v_{k_v}}(h-\kappa)}, \\
\mathbf{p}_{e,2} &= \sum_{k_v=1}^{2N} \varsigma_{k_v,N} \sum_{j=1}^{n+1} \gamma_{j,r+\alpha^v_{k_v}} \overline{\omega}'_{j,k_v} e^{\gamma_{j,r+\alpha^v_{k_v}}(h-\kappa)}, \\
\mathbf{p}_{e,4} &= \sum_{k_v=1}^{2N} \varsigma_{k_v,N} \left(\sum_{i=1}^{m+1} \underline{\omega}'_{i,k_v} - \sum_{j=1}^{n+1} \overline{\omega}'_{j,k_v} \right) \\
&\quad + \sum_{k_v=1}^{2N} \varsigma_{k_v,N} \left(\frac{\alpha^s_{k_s}}{\alpha^s_{k_s}+r} \frac{\alpha^v_{k_v}}{\alpha^v_{k_v}+r} e^{\kappa} - \frac{\alpha^s_{k_s}}{\alpha^s_{k_s}+\delta} \frac{\alpha^v_{k_v}}{\alpha^v_{k_v}+\delta} e^{\kappa} \right), \\
\mathbf{p}_{e,5} &= \sum_{k_v=1}^{2N} \varsigma_{k_v,N} \left(\sum_{i=1}^{m+1} \beta_{i,r+\alpha^v_{k_v}} \underline{\omega}'_{i,k_v} - \sum_{j=1}^{n+1} \gamma_{j,r+\alpha^v_{k_v}} \overline{\omega}'_{j,k_v} \right) \\
&\quad - \sum_{k_v=1}^{2N} \varsigma_{k_v,N} \frac{\alpha^s_{k_s}}{\alpha^s_{k_s}+\delta} \frac{\alpha^v_{k_v}}{\alpha^v_{k_v}+\delta} e^{\kappa}.
\end{aligned}
\tag{106}
$$

The elements $\mathbf{p}_{e,3}, \mathbf{p}_{e,7} \in \mathbb{R}^{1\times m}$ are defined (for $k = 1, .., m$) as

$$
\begin{aligned}
(\mathbf{p}_{e,3})_{1k} &= \sum_{k_v=1}^{2N} \varsigma_{k_v,N} \sum_{j=1}^{n+1} \frac{\overline{\omega}'_{j,k_v} e^{\gamma_{j,r+\alpha^s_{k_s}}(h-\kappa)}}{\eta_k - \gamma_{j,r+\alpha^v_{k_v}}}, \\
(\mathbf{p}_{e,7})_{1k} &= \sum_{k_v=1}^{2N} \varsigma_{k_v,N} \sum_{i=1}^{m+1} \frac{\underline{\omega}'_{i,k_v} e^{\eta_k(h-\kappa)}}{\eta_k - \beta_{i,r+\alpha^v_{k_v}}} \\
&\quad - \sum_{k_v=1}^{2N} \varsigma_{k_v,N} \sum_{j=1}^{n+1} \frac{\overline{\omega}'_{j,k_v} \left(e^{\eta_k(h-\kappa)} - e^{\gamma_{j,r+\alpha^v_{k_v}}(h-\kappa)} \right)}{\eta_k - \gamma_{j,r+\alpha^v_{k_v}}} \\
&\quad + \sum_{k_v=1}^{2N} \varsigma_{k_v,N} e^{\eta_k(h-\kappa)} \left(\frac{e^{\kappa}}{\eta_k} \frac{\alpha^s_{k_s}}{\alpha^s_{k_s}+r} \frac{\alpha^v_{k_v}}{\alpha^v_{k_v}+r} - \frac{e^{\kappa}}{\eta_k - 1} \frac{\alpha^s_{k_s}}{\alpha^s_{k_s}+\delta} \frac{\alpha^v_{k_v}}{\alpha^v_{k_v}+\delta} \right),
\end{aligned}
\tag{107}
$$

and the elements $\mathbf{p}_{e,6}, \mathbf{p}_{e,8} \in \mathbb{R}^{1\times n}$ are defined (for $l = 1, .., n$) as

$$
\begin{aligned}
(\mathbf{p}_{e,6})_{1l} &= \sum_{k_v=1}^{2N} \varsigma_{k_v,N} \left(\sum_{i=1}^{m+1} \frac{\underline{\omega}'_{i,k_v}}{\theta_l + \beta_{i,r+\alpha^v_{k_v}}} - \sum_{j=1}^{n+1} \frac{\overline{\omega}'_{j,k_v}}{\theta_l + \gamma_{j,r+\alpha^v_{k_v}}} \right) \\
&\quad + \sum_{k_v=1}^{2N} \varsigma_{k_v,N} \left(\frac{e^\kappa}{\theta_l} \frac{\alpha^s_{k_s}}{\alpha^s_{k_s}+r} \frac{\alpha^v_{k_v}}{\alpha^v_{k_v}+r} - \frac{e^\kappa}{\theta_l+1} \frac{\alpha^s_{k_s}}{\alpha^s_{k_s}+\delta} \frac{\alpha^v_{k_v}}{\alpha^v_{k_v}+\delta} \right), \\
(\mathbf{p}_{e,8})_{1l} &= \sum_{k_v=1}^{2N} \varsigma_{k_v,N} \sum_{i=1}^{m+1} \frac{\underline{\omega}'_{i,k_v} e^{\theta_l(\kappa-h)}}{\theta_l + \beta_{i,r+\alpha^v_{k_v}}} \\
&\quad + \sum_{k_v=1}^{2N} \varsigma_{k_v,N} \sum_{j=1}^{n+1} \frac{\overline{\omega}'_{j,k_v} \left(e^{\gamma_{j,r+\alpha^s_{k_s}}(h-\kappa)} - e^{\theta_l(\kappa-h)} \right)}{\theta_l + \gamma_{j,r+\alpha^v_{k_v}}} \\
&\quad + \sum_{k_v=1}^{2N} \varsigma_{k_v,N} e^{\theta_l(\kappa-h)} \left(\frac{e^\kappa}{\theta_l} \frac{\alpha^s_{k_s}}{\alpha^s_{k_s}+r} \frac{\alpha^v_{k_v}}{\alpha^v_{k_v}+r} - \frac{e^\kappa}{\theta_l+1} \frac{\alpha^s_{k_s}}{\alpha^s_{k_s}+\delta} \frac{\alpha^v_{k_v}}{\alpha^v_{k_v}+\delta} \right).
\end{aligned}
\tag{108}
$$

Finally, the $(2n + 2m + 4)$-dimensional square matrix $\mathbf{P}$ is given by

$$
\mathbf{P} := \begin{pmatrix}
\mathbf{P}_{11} & \mathbf{P}_{12} & \mathbf{P}_{13} & \mathbf{P}_{14} \\
\mathbf{P}_{21} & \mathbf{P}_{22} & \mathbf{P}_{23} & \mathbf{P}_{24} \\
\mathbf{P}_{31} & \mathbf{P}_{32} & \mathbf{P}_{33} & \mathbf{P}_{34} \\
\mathbf{P}_{41} & \mathbf{P}_{42} & \mathbf{P}_{43} & \mathbf{P}_{44} \\
\mathbf{P}_{51} & \mathbf{P}_{52} & \mathbf{P}_{53} & \mathbf{P}_{54} \\
\mathbf{P}_{61} & \mathbf{P}_{62} & \mathbf{P}_{63} & \mathbf{P}_{64} \\
\mathbf{P}_{71} & \mathbf{P}_{72} & \mathbf{P}_{73} & \mathbf{P}_{74} \\
\mathbf{P}_{81} & \mathbf{P}_{82} & \mathbf{P}_{83} & \mathbf{P}_{84}
\end{pmatrix},
\tag{109}
$$

where the elements of the matrix $\mathbf{P}$, i.e., the sub-matrices $\mathbf{P}_{kl}$ with $k = 1, ..., 8$ and $l = 1, ..., 4$, are given as follows.

1. For all $j = 1, ..., n + 1$, $\mathbf{P}_{11}, \mathbf{P}_{13}, \mathbf{P}_{21}, \mathbf{P}_{23}, \mathbf{P}_{41}, \mathbf{P}_{43}, \mathbf{P}_{51}, \mathbf{P}_{53} \in \mathbb{R}^{1\times(n+1)}$ are:

   $(\mathbf{P}_{11})_{1j} = -(\mathbf{P}_{13})_{1j} = 1$, $(\mathbf{P}_{21})_{1j} = \gamma_{j,r+\alpha^e_{k_e}}$, $(\mathbf{P}_{23})_{1j} = -\gamma_{j,r+\alpha^s_{k_s}}$, $(\mathbf{P}_{41})_{1j} = (\mathbf{P}_{51})_{1j} = 0$, $(\mathbf{P}_{43})_{1j} = e^{\gamma_{j,r+\alpha^s_{k_s}}(\kappa-h)}$, and $(\mathbf{P}_{53})_{1j} = \gamma_{j,r+\alpha^s_{k_s}} e^{\gamma_{j,r+\alpha^s_{k_s}}(\kappa-h)}$.

2. For all $j = 1, ..., m + 1$, $\mathbf{P}_{12}, \mathbf{P}_{14}, \mathbf{P}_{22}, \mathbf{P}_{24}, \mathbf{P}_{42}, \mathbf{P}_{44}, \mathbf{P}_{52}, \mathbf{P}_{54} \in \mathbb{R}^{1\times(m+1)}$ are:

   $(\mathbf{P}_{12})_{1j} = (\mathbf{P}_{44})_{1j} = -1$, $(\mathbf{P}_{14})_{1j} = (\mathbf{P}_{24})_{1j} = 0$, $(\mathbf{P}_{22})_{1j} = -\beta_{j,r+\alpha^e_{k_e}}$, $(\mathbf{P}_{42})_{1j} = e^{\beta_{j,r+\alpha^s_{k_s}}(\kappa-h)}$, $(\mathbf{P}_{52})_{1j} = \beta_{j,r+\alpha^s_{k_s}} e^{\beta_{j,r+\alpha^s_{k_s}}(\kappa-h)}$, and $(\mathbf{P}_{54})_{1j} = -\beta_{j,r+\alpha^s_{k_s}}$.

3. For $i = 1, ..., m$ and $j = 1, ..., n + 1$, $\mathbf{P}_{31}, \mathbf{P}_{33}, \mathbf{P}_{71}, \mathbf{P}_{73} \in \mathbb{R}^{m\times(n+1)}$ are:

$(\mathbf{P}_{31})_{ij} = (\mathbf{P}_{71})_{ij} = 1/(\eta_i - \gamma_{j,r+\alpha^e_{k_e}})$, $(\mathbf{P}_{33})_{ij} = -1/(\eta_i - \gamma_{j,r+\alpha^s_{k_s}})$, and $(\mathbf{P}_{73})_{ij} = -\left(1 - e^{(\eta_i - \gamma_{j,r+\alpha^s_{k_s}})(h-\kappa)}\right)/(\eta_i - \gamma_{j,r+\alpha^s_{k_s}})$.

4. For $i = 1, ..., m$ and $j = 1, ..., m+1$, $\mathbf{P}_{32}, \mathbf{P}_{34}, \mathbf{P}_{72}, \mathbf{P}_{74} \in \mathbb{R}^{m\times(m+1)}$ are:

   $(\mathbf{P}_{32})_{ij} = -1/(\eta_i - \beta_{j,r+\alpha^s_{k_s}})$, $(\mathbf{P}_{34})_{ij} = 0$, $(\mathbf{P}_{72})_{ij} = -\left(1 - e^{(\eta_i - \beta_{j,r+\alpha^s_{k_s}})(h-\kappa)}\right)/(\eta_i - \beta_{j,r+\alpha^s_{k_s}})$, and $(\mathbf{P}_{74})_{ij} = -e^{\eta_i(h-\kappa)}/(\eta_i - \beta_{j,r+\alpha^s_{k_s}})$.

5. For $i = 1, ..., n$ and $j = 1, ..., n+1$, $\mathbf{P}_{61}, \mathbf{P}_{63}, \mathbf{P}_{81}, \mathbf{P}_{83} \in \mathbb{R}^{n\times(n+1)}$ are:

   $(\mathbf{P}_{61})_{ij} = 0$, $(\mathbf{P}_{63})_{ij} = e^{\gamma_{j,r+\alpha^s_{k_s}}(\kappa-h)}/(\theta_i + \gamma_{j,r+\alpha^s_{k_s}})$, $(\mathbf{P}_{81})_{ij} = 1/(\theta_i + \gamma_{j,r+\alpha^e_{k_e}})$, and $(\mathbf{P}_{83})_{ij} = -\left(1 - e^{(\theta_i + \gamma_{j,r+\alpha^s_{k_s}})(\kappa-h)}\right)/(\theta_i + \gamma_{j,r+\alpha^s_{k_s}})$.

6. For $i = 1, ..., n$ and $j = 1, ..., m+1$, $\mathbf{P}_{62}, \mathbf{P}_{64}, \mathbf{P}_{82}, \mathbf{P}_{84} \in \mathbb{R}^{n\times(m+1)}$ are:

   $(\mathbf{P}_{62})_{ij} = e^{\beta_{j,r+\alpha^s_{k_s}}(\kappa-h)}/(\theta_i + \beta_{j,r+\alpha^s_{k_s}})$, $(\mathbf{P}_{64})_{ij} = -1/(\theta_i + \beta_{j,r+\alpha^s_{k_s}})$, $(\mathbf{P}_{82})_{ij} = -\left(1 - e^{(\theta_i + \beta_{j,r+\alpha^s_{k_s}})(\kappa-h)}\right)/(\theta_i + \beta_{j,r+\alpha^s_{k_s}})$, and $(\mathbf{P}_{84})_{ij} = -e^{\theta_i(\kappa-h)}/(\theta_i + \beta_{j,r+\alpha^s_{k_s}})$.

■

Appendix B Pricing of Québécoised American Parisian put options: Proof of Theorem 2

Using the same change of variables as in Appendix A the equation (57) becomes

$$\begin{cases} -\dfrac{\partial \tilde{\epsilon}_{uo}}{\partial \tau_e}(x, \tau_s, \tau_e) + \mathcal{L}\tilde{\epsilon}_{uo}(x, \tau_s, \tau_e) = r\tilde{\epsilon}_{uo}(x, \tau_s, \tau_e), & \text{if } (x, t_s, t_e) \in \tilde{\mathscr{E}}, \\ -\dfrac{\partial \tilde{\epsilon}_{uo}}{\partial \tau_s}(x, \tau_s, \tau_e) + \mathcal{L}\tilde{\epsilon}_{uo}(x, \tau_s, \tau_e) = r\tilde{\epsilon}_{uo}(x, t_s, t_e), & \text{if } (x, \tau_s, \tau_e) \in \tilde{\mathscr{S}}^*. \end{cases} \tag{110}$$

Similarly, we adjust the notation in the equations (58)–(61). The DLCT of our PIDE system for the early exercise premium gives us two coupled OIDEs, which can be solved analytically. In the standard continuation region $\tilde{\mathscr{S}}^*$ the OIDE describing the dynamics of the québécoised early exercise premium of the Parisian up-and-out put option is

$$\begin{aligned} \frac{\sigma^2}{2}\frac{d^2\hat{\tilde{\epsilon}}_{uo}}{dx^2}(x, \alpha^s_{k_s}, \alpha^e_{k_e}) + \mu\frac{d\hat{\tilde{\epsilon}}_{uo}}{dx}(x, \alpha^s_{k_s}, \alpha^e_{k_e}) - (r + \alpha^s_{k_s} + \lambda)\hat{\tilde{\epsilon}}_{uo}(x, \alpha^s_{k_s}, \alpha^e_{k_e}) \\ + \alpha^s_{k_s}\epsilon_p(x, D) + \lambda\int_{-\infty}^{+\infty}\hat{\tilde{\epsilon}}_{uo}(x + y, \alpha^s_{k_s}, \alpha^e_{k_e})\varphi_Y(y)dy = 0, \end{aligned} \tag{111}$$

where $\epsilon_p(x,D) := P(x,D) - p(x,D)$ is the early exercise premium of the vanilla American option. On the other hand, in the excursion region $\tilde{\mathscr{E}}$ we have

$$\begin{aligned}\frac{\sigma^2}{2}\frac{d^2\hat{\tilde{\epsilon}}_{uo}}{dx^2}(x,\alpha^s_{k_s},\alpha^e_{k_e}) + \mu\frac{d\hat{\tilde{\epsilon}}_{uo}}{dx}(x,\alpha^s_{k_s},\alpha^e_{k_e}) - (r+\alpha^e_{k_e}+\lambda)\hat{\tilde{\epsilon}}_{uo}(x,\alpha^s_{k_s},\alpha^e_{k_e}) \\ + \lambda\int_{-\infty}^{+\infty}\hat{\tilde{\epsilon}}_{uo}(x+y,\alpha^s_{k_s},\alpha^e_{k_e})\varphi_Y(y)dy = 0.\end{aligned} \tag{112}$$

The initial conditions in the standard continuation and the excursion region are incorporated in the OIDEs. The boundary condition in the québécoised excursion region is

$$\lim_{x\uparrow+\infty}\hat{\tilde{\epsilon}}^e_{uo}(x,\alpha^e_{k_e}) = 0, \tag{113}$$

whereas the transformed boundary conditions between the excursion and the standard continuation region are

$$\begin{aligned}\lim_{x\uparrow h}\hat{\tilde{\epsilon}}^s_{uo}(x,\alpha^s_{k_s}) &= \lim_{x\downarrow h}\hat{\tilde{\epsilon}}^e_{uo}(x,\alpha^e_{k_e}), \\ \lim_{x\uparrow h}\frac{\partial\hat{\tilde{\epsilon}}^s_{uo}}{\partial x}(x,\alpha^s_{k_s}) &= \lim_{x\downarrow h}\frac{\partial\hat{\tilde{\epsilon}}^e_{uo}}{\partial x}(x,\alpha^e_{k_e}).\end{aligned} \tag{114}$$

Finally, the transformed value-matching and smooth pasting conditions at the boundary between the standard continuation and the exercise region are

$$\begin{aligned}\lim_{x\downarrow\hat{b}}\hat{\tilde{\epsilon}}^s_{uo}(x,\alpha^s_{k_s}) &= e^{\kappa} - e^{\hat{b}} - \hat{\tilde{\pi}}^s_{uo}(x,\alpha^s_{k_s})\big|_{x=\hat{b}}, \\ \lim_{x\downarrow\hat{b}}\frac{\partial\hat{\tilde{\epsilon}}^s_{uo}}{\partial x}(x,\alpha^s_{k_s}) &= -e^{\hat{b}} - \frac{\partial\hat{\tilde{\pi}}^s_{uo}}{\partial x}(x,\alpha^s_{k_s})\Big|_{x=\hat{b}}.\end{aligned} \tag{115}$$

Using the ansatz (62)–(64) to solve the system of OIDEs given above and following the same computational procedure as in the case of European Parisian up-and-out put option—which we omit here for brevity—we obtain the following matrix equation for the unknown coefficients

$$\mathbf{Q}\mathbf{u}_a = \mathbf{p}_a. \tag{116}$$

The vector $\mathbf{u}_a$ is given by $\mathbf{u}_a := (\mathbf{d}^-, \mathbf{f}^+, \mathbf{f}^-)'$ where $\mathbf{d}^- := (D^-_1, ..., D^-_{n+1})'$, $\mathbf{f}^+ := (F^+_1, ..., F^+_{m+1})'$, and $\mathbf{f}^- := (F^-_1, ..., F^-_{n+1})'$. The $(m+2n+3)$-dimensional column vector $\mathbf{p}_a$ is defined as $\mathbf{p}_a := (\mathbf{p}_{a,1}, \mathbf{p}_{a,2}, \mathbf{p}_{a,3}, \mathbf{p}_{a,4}, \mathbf{p}_{a,5}, \mathbf{p}_{a,6})'$.

The elements $\mathbf{p}_{a,1}, \mathbf{p}_{a,2}, \mathbf{p}_{a,4} \in \mathbb{R}^{1\times 1}$ are

$$\begin{aligned}
\mathbf{p}_{a,1} &= \sum_{k_v=1}^{2N} \varsigma_{k_v,N} \sum_{j=1}^{n+1} \varphi'_{j,k_v} e^{\gamma_{j,r+\alpha^v_{k_v}}(h-\hat{b})}, \\
\mathbf{p}_{a,2} &= \sum_{k_v=1}^{2N} \varsigma_{k_v,N} \sum_{j=1}^{n+1} \gamma_{j,r+\alpha^v_{k_v}} \varphi'_{j,k_v} e^{\gamma_{j,r+\alpha^v_{k_v}}(h-\hat{b})}, \\
\mathbf{p}_{a,4} &= \sum_{k_v=1}^{2N} \varsigma_{k_v,N} \sum_{j=1}^{n+1} \varphi'_{j,k_v} + \sum_{i=1}^{m+1} C_i^+ e^{\beta_{i,r+\alpha^s_{k_s}}(\hat{b}-\kappa)} + \sum_{k_v=1}^{2N} \varsigma_{k_v,N} \sum_{i=1}^{m+1} \underline{w}'_{i,k_v} e^{\beta_{i,r+\alpha^v_{k_v}}(\hat{b}-\kappa)} \\
&\quad - \sum_{k_v=1}^{2N} \varsigma_{k_v,N} \left(1 - \frac{\alpha^s_{k_s}}{\alpha^s_{k_s}+r} \frac{\alpha^v_{k_v}}{\alpha^v_{k_v}+r}\right) e^{\kappa} + \sum_{k_v=1}^{2N} \varsigma_{k_v,N} \left(1 - \frac{\alpha^s_{k_s}}{\alpha^s_{k_s}+\delta} \frac{\alpha^v_{k_v}}{\alpha^v_{k_v}+\delta}\right) e^{\hat{b}}.
\end{aligned} \tag{117}$$

The element $\mathbf{p}_{a,5} \in \mathbb{R}^{1\times m}$ is given (for $k = 1, .., m$) by

$$(\mathbf{p}_{a,5})_{1k} = \sum_{k_v=1}^{2N} \varsigma_{k_v,N} \sum_{j=1}^{n+1} \frac{\underline{w}'_{j,k_v} e^{\gamma_{j,r+\alpha^v_{k_v}}(h-\kappa)}}{\eta_k - \gamma_{j,r+\alpha^v_{r+k_v}}}, \tag{118}$$

and the elements $\mathbf{p}_{a,3}, \mathbf{p}_{a,6} \in \mathbb{R}^{1\times n}$ are defined (for $l = 1, .., n$) as

$$\begin{aligned}
(\mathbf{p}_{a,3})_{1l} &= \sum_{k_v=1}^{2N} \varsigma_{k_v,N} \sum_{j=1}^{n+1} \frac{\varphi'_{j,k_v} \left(e^{\gamma_{j,r+\alpha^v_{k_v}}(h-\hat{b})} - e^{\theta_l(\hat{b}-h)}\right)}{\theta_l + \gamma_{j,r+\alpha^v_{r+k_v}}} \\
&\quad - \sum_{i=1}^{m+1} \frac{C_i^+ e^{\beta_{i,r+\alpha^s_{k_s}}(\hat{b}-\kappa)+\theta_l(\hat{b}-h)}}{\theta_l + \beta_{i,r+\alpha^s_{k_s}}} \\
&\quad - \sum_{k_v=1}^{2N} \varsigma_{k_v,N} \sum_{i=1}^{m+1} \frac{\underline{w}'_{i,k_v} e^{\beta_{i,r+\alpha^v_{k_v}}(\hat{b}-\kappa)+\theta_l(\hat{b}-h)}}{\theta_l + \beta_{i,r+\alpha^v_{k_v}}} \\
&\quad + \sum_{k_v=1}^{2N} \varsigma_{k_v,N} e^{\theta_l(\hat{b}-h)} \left(1 - \frac{\alpha^s_{k_s}}{\alpha^s_{k_s}+r} \frac{\alpha^v_{k_v}}{\alpha^v_{k_v}+r}\right) \frac{e^{\kappa}}{\theta_l} \\
&\quad - \sum_{k_v=1}^{2N} \varsigma_{k_v,N} e^{\theta_l(\hat{b}-h)} \left(1 - \frac{\alpha^s_{k_s}}{\alpha^s_{k_s}+\delta} \frac{\alpha^v_{k_v}}{\alpha^v_{k_v}+\delta}\right) \frac{e^{\hat{b}}}{\theta_l+1}, \\
(\mathbf{p}_{a,6})_{1l} &= (\mathbf{p}_{a,3})_{1l} - \sum_{k_v=1}^{2N} \varsigma_{k_v,N} \sum_{j=1}^{n+1} \frac{\varphi'_{j,k_v} e^{\gamma_{j,r+\alpha^v_{k_v}}(h-\hat{b})}}{\theta_l + \gamma_{j,r+\alpha^v_{r+k_v}}}.
\end{aligned} \tag{119}$$

Finally, the $(m+2n+3)$-dimensional square matrix $\mathbf{Q}$ is given by

$$\mathbf{Q} := \begin{pmatrix} \mathbf{Q}_{11} & \mathbf{Q}_{12} & \mathbf{Q}_{13} \\ \mathbf{Q}_{21} & \mathbf{Q}_{22} & \mathbf{Q}_{23} \\ \mathbf{Q}_{31} & \mathbf{Q}_{32} & \mathbf{Q}_{33} \\ \mathbf{Q}_{41} & \mathbf{Q}_{42} & \mathbf{Q}_{43} \\ \mathbf{Q}_{51} & \mathbf{Q}_{52} & \mathbf{Q}_{53} \\ \mathbf{Q}_{61} & \mathbf{Q}_{62} & \mathbf{Q}_{63} \end{pmatrix}, \tag{120}$$

where the elements of the matrix $\mathbf{Q}$, i.e., the sub-matrices $\mathbf{Q}_{kl}$ with $k = 1, ..., 6$ and $l = 1, 2, 3$, are given below.

1. For all $j = 1, ..., n+1$, $\mathbf{Q}_{11}, \mathbf{Q}_{13}, \mathbf{Q}_{21}, \mathbf{Q}_{23}, \mathbf{Q}_{41}, \mathbf{Q}_{43} \in \mathbb{R}^{1\times(n+1)}$ are:

   $(\mathbf{Q}_{11})_{1j} = -(\mathbf{Q}_{13})_{1j} = 1$, $(\mathbf{Q}_{21})_{1j} = \gamma_{j,r+\alpha^e_{k_e}}$, $(\mathbf{P}_{23})_{1j} = -\gamma_{j,r+\alpha^s_{k_s}}$, $(\mathbf{Q}_{41})_{1j} = 0$, and $(\mathbf{Q}_{43})_{1j} = -e^{\gamma_{j,r+\alpha^s_{k_s}}(\hat{b}-\kappa)}$.

2. For all $j = 1, ..., m+1$, $\mathbf{Q}_{12}, \mathbf{Q}_{22}, \mathbf{Q}_{42} \in \mathbb{R}^{1\times(m+1)}$ are:

   $(\mathbf{Q}_{12})_{1j} = -1$, $(\mathbf{Q}_{22})_{1j} = -\beta_{j,r+\alpha^s_{k_s}}$, and $(\mathbf{Q}_{42})_{1j} = -e^{\beta_{j,r+\alpha^s_{k_s}}(\hat{b}-\kappa)}$.

3. For $i = 1, ..., m$ and $j = 1, ..., n+1$, $\mathbf{Q}_{51}, \mathbf{Q}_{53} \in \mathbb{R}^{m\times(n+1)}$ are:

   $(\mathbf{Q}_{51})_{ij} = 1/(\eta_i - \gamma_{j,r+\alpha^e_{k_e}})$, and $(\mathbf{Q}_{53})_{ij} = -1/(\eta_i - \gamma_{j,r+\alpha^s_{k_s}})$.

4. For $i = 1, ..., m$ and $j = 1, ..., m+1$, $\mathbf{Q}_{52} \in \mathbb{R}^{m\times(m+1)}$ are:

   $(\mathbf{Q}_{52})_{ij} = -1/(\eta_i - \beta_{j,r+\alpha^s_{k_s}})$.

5. For $i = 1, ..., n$ and $j = 1, ..., n+1$, $\mathbf{Q}_{31}, \mathbf{Q}_{33}, \mathbf{Q}_{61}, \mathbf{Q}_{63} \in \mathbb{R}^{n\times(n+1)}$ are:

   $(\mathbf{Q}_{31})_{ij} = 1/(\theta_i + \gamma_{j,r+\alpha^e_{k_e}})$, $(\mathbf{Q}_{33})_{ij} = -\left(1 - e^{(\theta_i+\gamma_{j,r+\alpha^s_{k_s}})(\hat{b}-h)}\right)/(\theta_i + \gamma_{j,r+\alpha^s_{k_s}})$, $(\mathbf{Q}_{63})_{ij} = e^{(\theta_i+\gamma_{j,r+\alpha^s_{k_s}})(\hat{b}-h)}/(\theta_i + \gamma_{j,r+\alpha^s_{k_s}})$ and $(\mathbf{Q}_{61})_{ij} = 0$.

6. For $i = 1, ..., n$ and $j = 1, ..., m+1$, $\mathbf{Q}_{32}, \mathbf{Q}_{62} \in \mathbb{R}^{n\times(m+1)}$ are:

   $(\mathbf{Q}_{32})_{ij} = -\left(1 - e^{(\theta_i+\beta_{j,r+\alpha^s_{k_s}})(\hat{b}-h)}\right)/(\theta_i+\beta_{j,r+\alpha^s_{k_s}})$, and $(\mathbf{Q}_{62})_{ij} = e^{(\theta_i+\beta_{j,r+\alpha^s_{k_s}})(\hat{b}-h)}/(\theta_i+\beta_{j,r+\alpha^s_{k_s}})$.

   The québécoised early exercise boundary can be computed using the second equation in (115).

■